



특론: 가속기 실험실습 I

(NUCE719P-01/PHYS715P-01, 정모세)

소각 X-선 소각 산란 개요 및 활용

진 경 식

첨단원자력공학부

jinks@postech.ac.kr, PAL 저장링동 224호



장치소개

방사광가속기란

What is a Synchrotron Light Source?

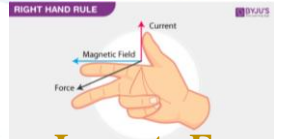
방사광가속기란 빠르게 움직이는 전자가 빔관을 통해 제 1진동현상으로 발생한 방사광은 물질구조를 분석하거나 미세구조 등에 활용된다. 2세대 방사광가속기가 미국전지역에서 발생하는 방사광을 목적으로 개발된 데 반하여 4세대 방사광 가속기는 미국전지역뿐만 아니라 설립국에서는 특수하게 배열된 저장링에서 저장링의 직선 구간에서 발생하여 보다 우수한 방사광을 만들고 있다.

방사광 가속기 구조

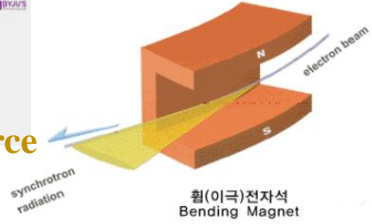
- 전자가 빛의 속도로 달리게 해주는 선형가속기
- 빛을 받아내는 저장링
- 빛이난 빛으로 다양한 연구를 하는 빔라인

Synchrotron Light Source is a facility that uses the light emitted in the tangential direction when fast-moving electrons move in a circle. The light can be used for analyses of material structures, ultra-fine lithography, and so on. In contrast to 2 generation light source built for the purpose of radiation generated from bending magnets, 3 generation light source produces higher-quality radiation based on special electromagnets, or insertion devices, installed in the straight sections of the storage rings as well as the bending magnets.

RIGHT HAND RULE



Lorentz Force



힘(이국)전자석 Bending Magnet

3 빔라인 Beamlines

전자가 저장링에서 회전하면서 발생하는 방사광을 사용자들이 있는 곳까지 전달하는 관9000, 8000인 빛을 통로로 목적에 맞게 세팅 장소까지 이끔이 주어 실험실의 환경, 그들을 유기 고분자 재료까지 세포 연구, 미생으로 의학용 효소, 신약 개발 등 다양한 분야에서 다양한 연구가 이루어지도록 한다.

Beamlines guide the synchrotron radiation emitted from electrons in the storage ring to the experimental area. Various kinds of application research can be done in a variety of fields such as new material alloys, high-efficiency organic molecules for solar cells, micro robots for medical operations, development of new medicines.

2 Storage ring 저장링

선형가속기에서 광속에 가깝게 가속 된 전자는 둘레길이 281.8m 원형의 저장링에서 10시간 이상 저장되고 돌게 된다.

Once electrons are accelerated close to the speed of light inside the linear accelerator, they are to rotate for over 10 hours inside the 280 m long storage ring.

Magnets 자석 장치

전자 통로 안에는 24개의 이국전지역이 20미터 전자가 이국전지역을 2년 데이다 15도 제 방향을 바꾸어 광을 속도 높게 한다. 또한 4극 전지역 및 6극 전지역으로 전자가 안정된 궤도를 속도 높게 만든다.

Inside electronic pathways there are 24 bending magnets. Every time electrons pass through the bending magnets, they change direction by an angle of 15 degrees and make a circular orbit. Further, the quadrupole and sextupole magnets enable electrons to keep stable orbits.

이국전지역 저장링을 회전하는 전자가 이국전지역에서 세이브 역할에 관여한다.

삽입장치 저장링을 회전하는 전자가 삽입장치를 통과하면서 제3세대 방사광을 만들어낸다.

Bending magnets Synchrotron radiation is generated when electrons rotating inside the storage ring pass through the bending magnets.

Insertion devices Electrons rotating in the storage ring produce 3rd generation synchrotron radiation while passing through the insertion devices.



1 선형가속기 Linear accelerator

- PLS-II 선형가속기는 계속 빔에너지가 3 GeV 이고 저장링에 전자를 입사하는 방사광의 역할을 한다. 선형가속기의 전체 길이는 약 170m 이고 지중 8m 깊이에 설치되어 있으며, 선형가속기에서 가속된 전자는 Beam Transport Line을 지나서 저장링에 들어간다.
- PLS-II linear accelerator accelerates electrons up to 3 GeV energy and injects them into the storage ring installed in a tunnel five underground. The linear accelerator measures approx. 170 m in its total length. Electrons accelerated inside the linear accelerator pass through the Beam Transport Line before entering the storage ring as incident beams.





Radio-frequency cavities 고주파 공진기

고주파 공진기는 전자가 저장링을 돌면서 잃어버리는 에너지를 보충해 주는 역할을 한다. 현재 3개의 초전도 공진기가 운영 중이다.

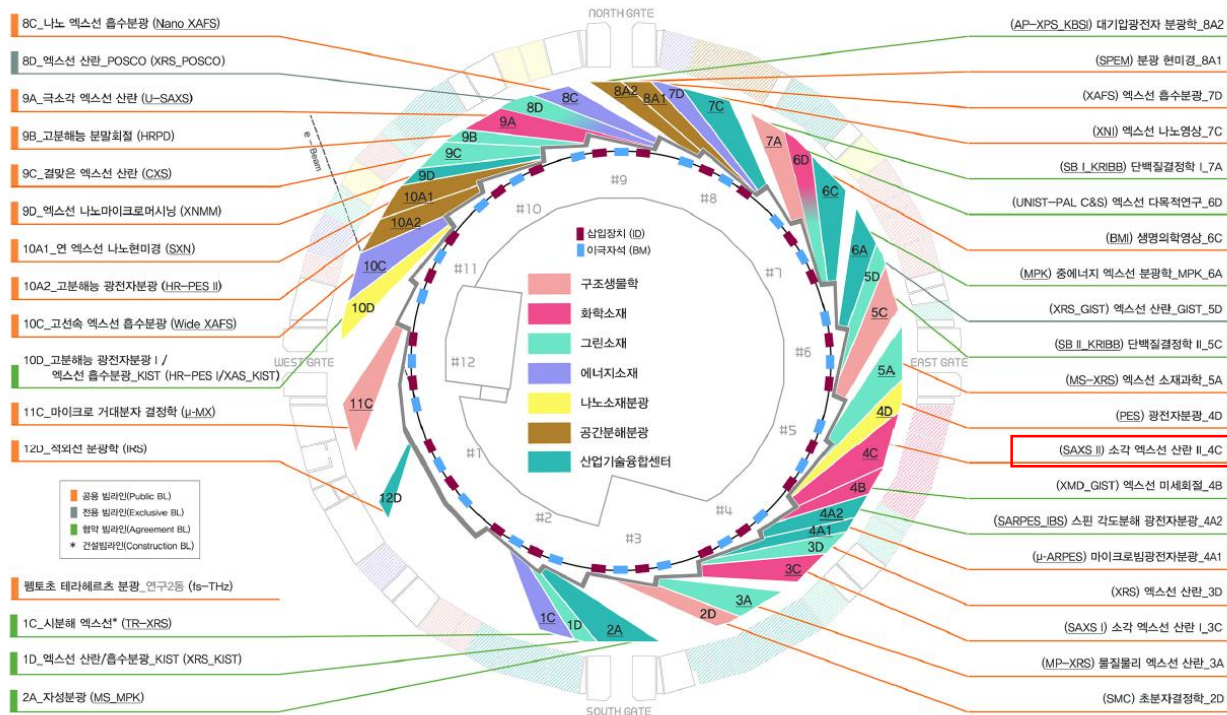
Radio-frequency cavities make up for energy that electrons lose while circulating throughout the storage rings. 3 superconducting cavities are in operation.



3세대 빔라인 현황 (36기)

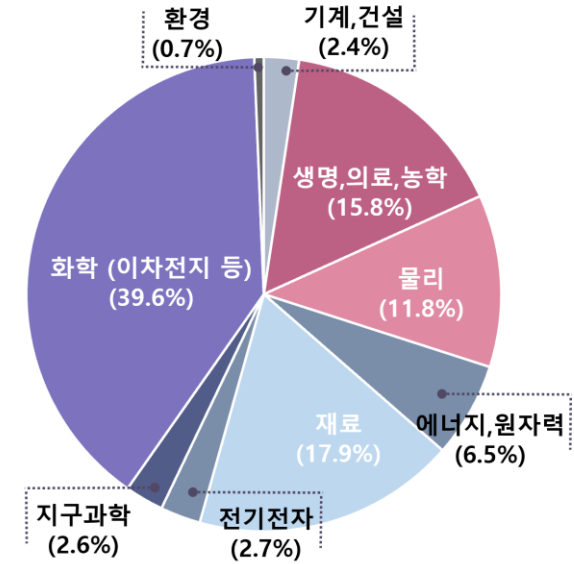
Storage Ring

- Electron beam energy: 3 GeV
- Ring current: 400 mA, Top-up mode
- User beamtime: 190 days/year



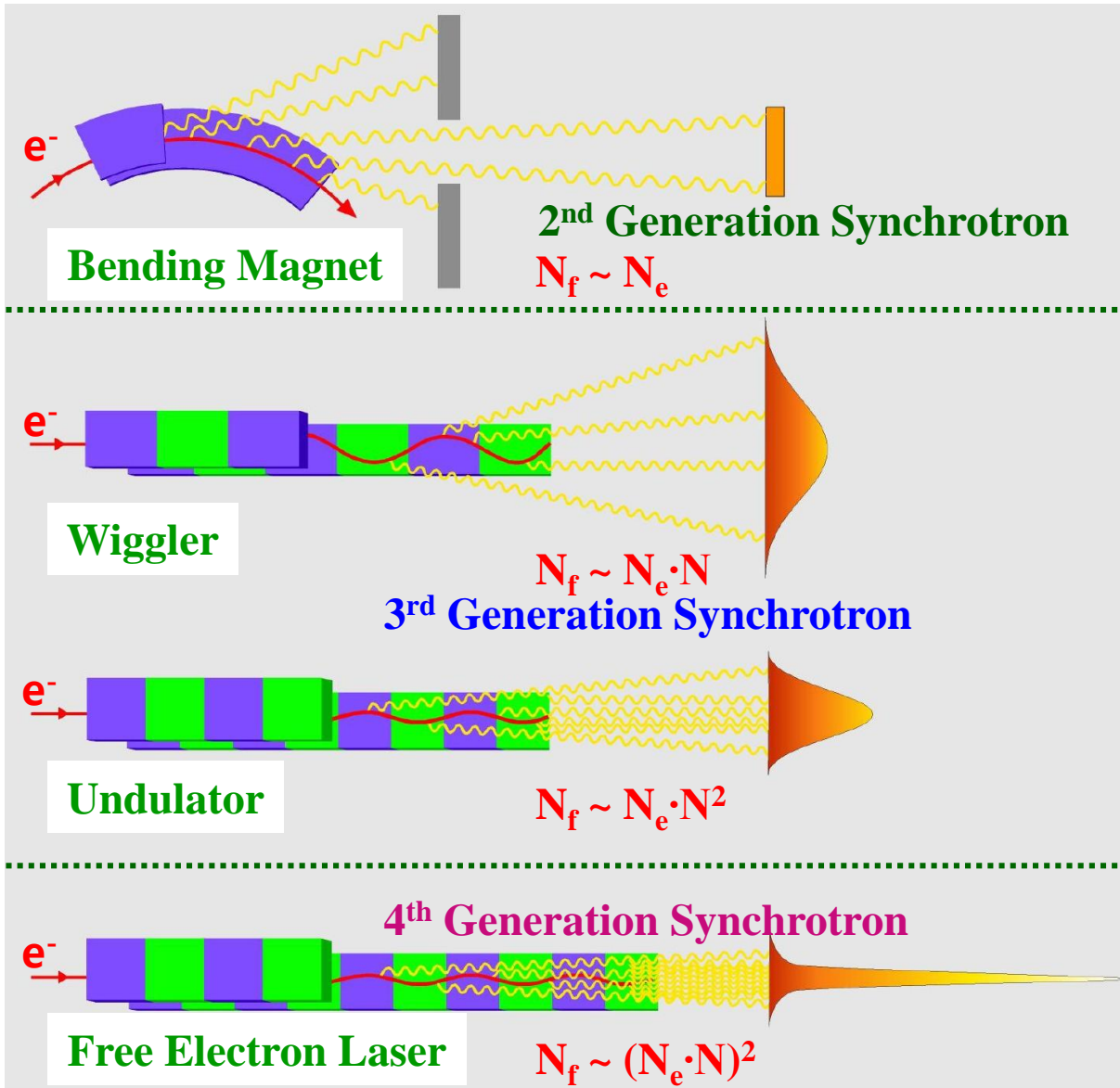
3세대 연구분야

▶ '22년 배정 기준



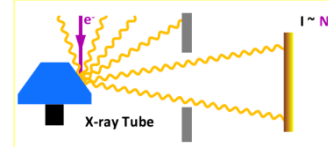
3세대 사용기관 (배정)

구분	국 내			외국	계
	대학	연구소	산업체		
'21	1,539 (82.3%)	234 (12.5%)	52 (2.8%)	46 (2.4%)	1,871
'22	1,691 (84.2%)	220 (11.0%)	73 (3.6%)	25 (1.2%)	2,009



Synchrotron radiation is produced when particles are **accelerated** in a storage ring.

N_f : the number of radiated photons
 N_e : the number of electrons in the beam
 N : the number of undulator periods



Wiggler and undulator - linear magnetic structures - are used to improve the properties of the radiation produced.

Direct descendants of the bending magnets in a storage ring, wiggler and undulator, force the particles to travel along a zig-zag path so that the emitted light waves are **superimposed**.

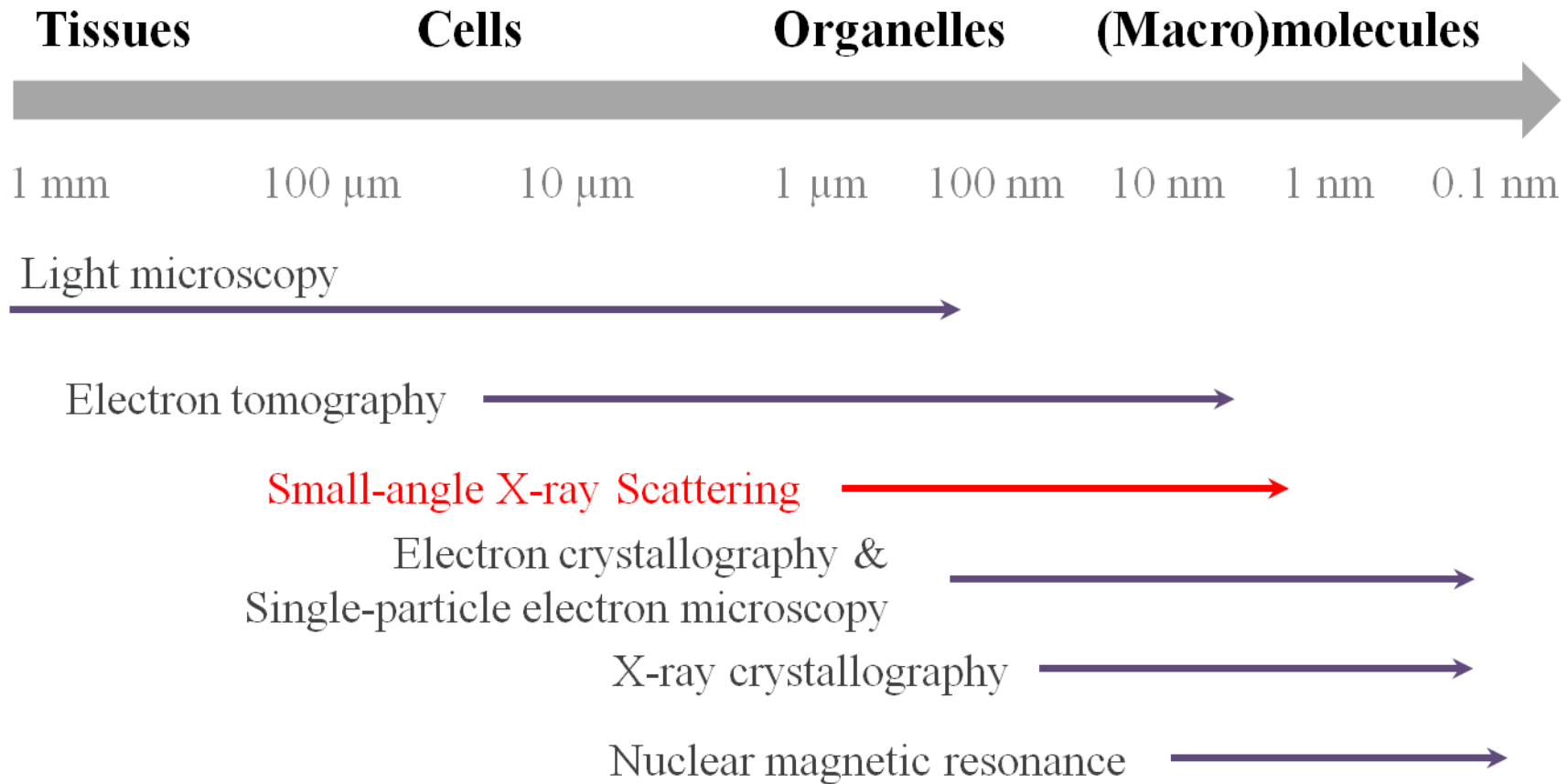
These magnetic structures are now used to produce synchrotron radiation in laboratories worldwide. Extremely intense X-ray radiation with laser-like properties is generated by free-electron lasers.

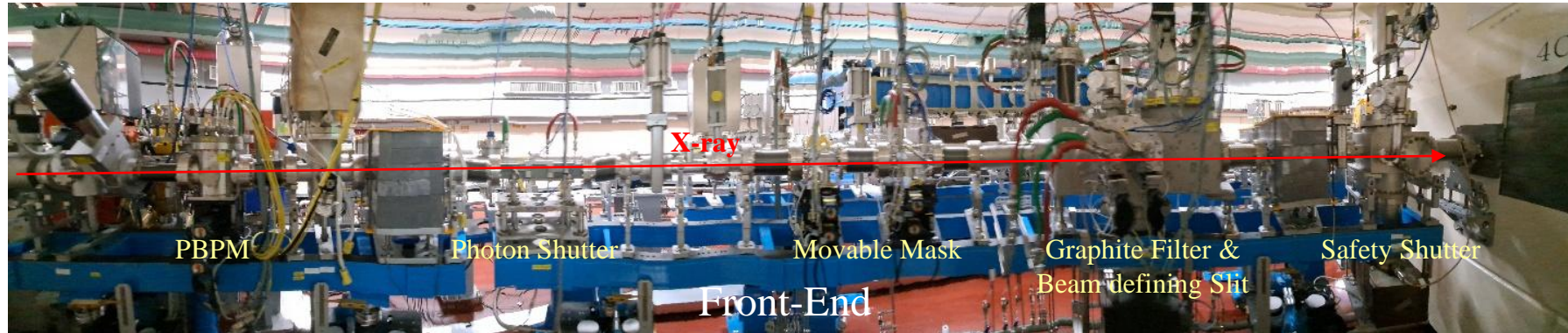
- ❖ SAXS is a **fundamental and powerful tool** for structural analyses of polymers, metals, alloys, liquid crystals, and colloidal systems.
 - ❖ Synchrotron radiation X-ray sources with a **high-flux photon and low-divergence beam** enable broader application of SAXS, such as time-resolved measurements of powder/film samples in solid and nanoparticles/biomacromolecules in solution.
 - ❖ SAXS is becoming a **standard tool** for the structural characterization under carefully controlled conditions, such as pH, ionic strength, chemical reagents, humidity, electric/magnet field, pressure, and temperature.
- ✓ **Beamlines currently in operation at PAL: 3C SAXS I, 4C SAXS II, 6D UNIST-PAL, and 9A U-SAXS**

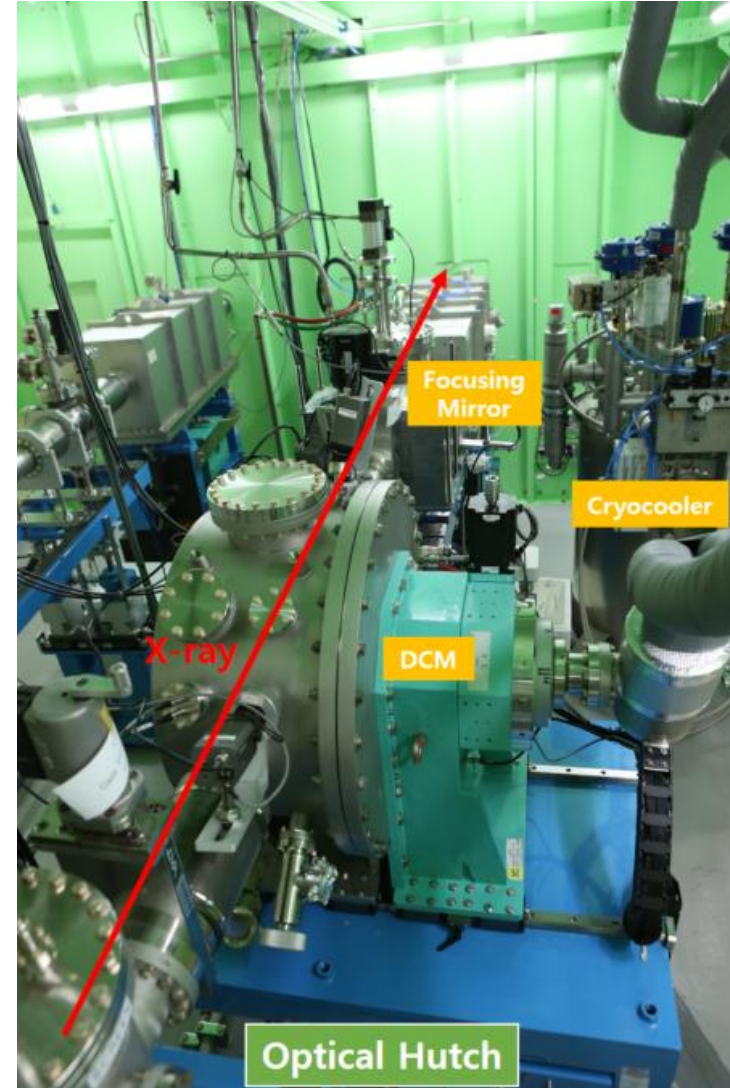
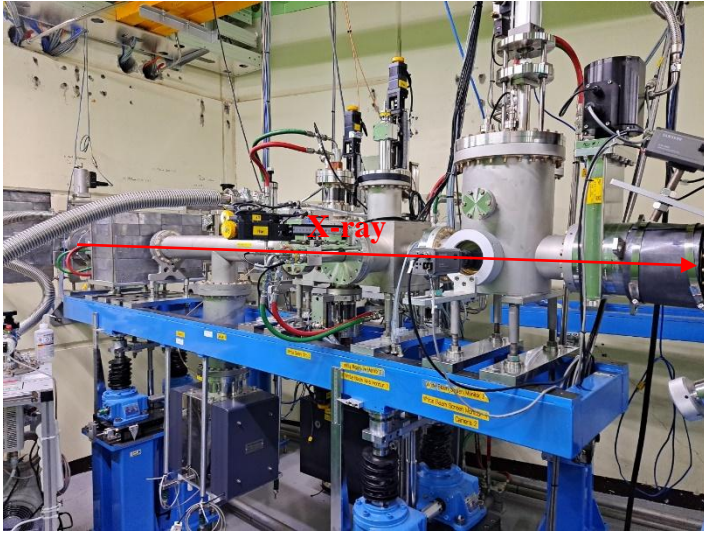
Applications

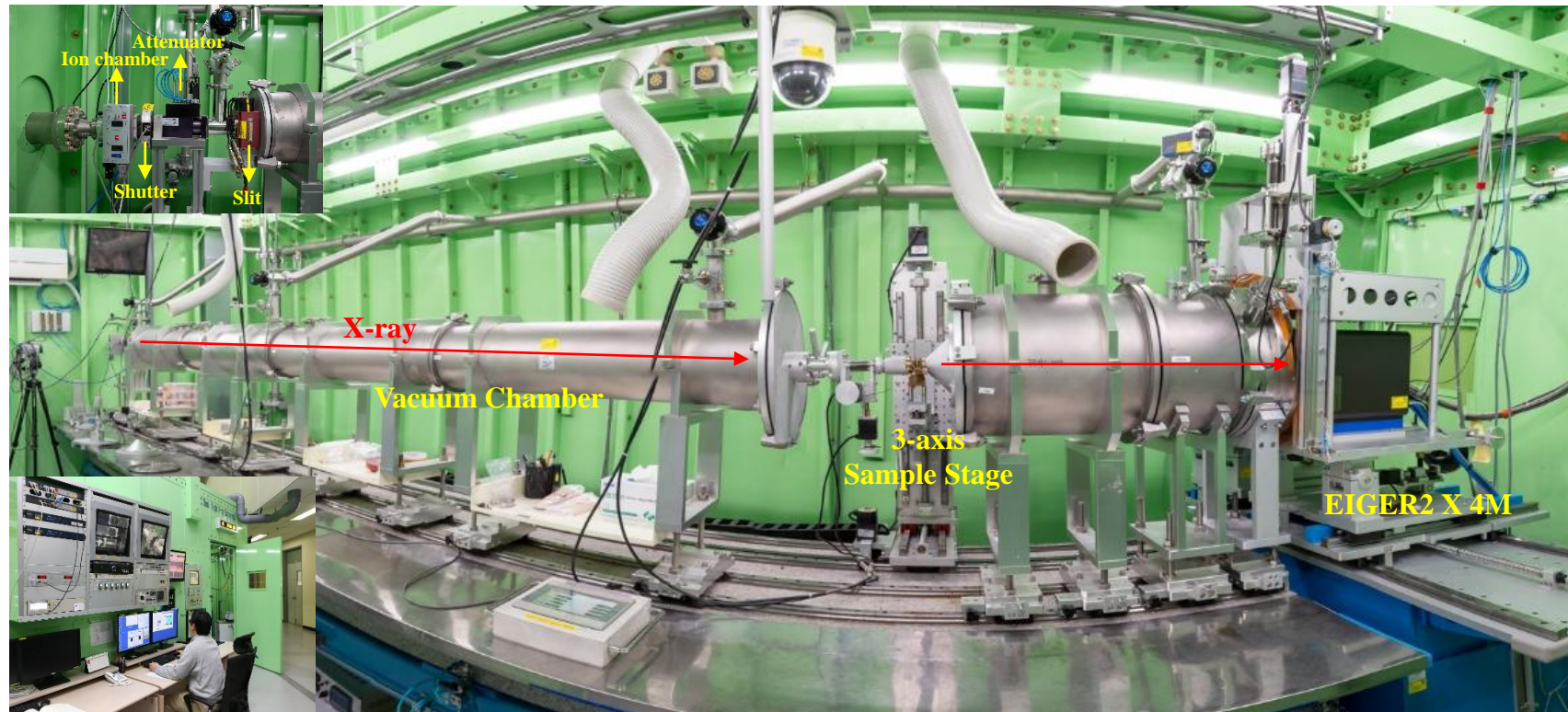
SAXS is used for the determination of nanoscale structure of particle systems

- Energy Material: Organic Solar Cell, Battery
- Flexible Display: Organic Thin-film Transistor
- Ultra Low-k Dielectric Material
- Nano-template Fabrication
- Micro-array Fabrication
- Synthetic Polymer Nanostructure Studies
- Biological Nanostructure Studies (Protein, DNA, Drug Delivery System, etc.)







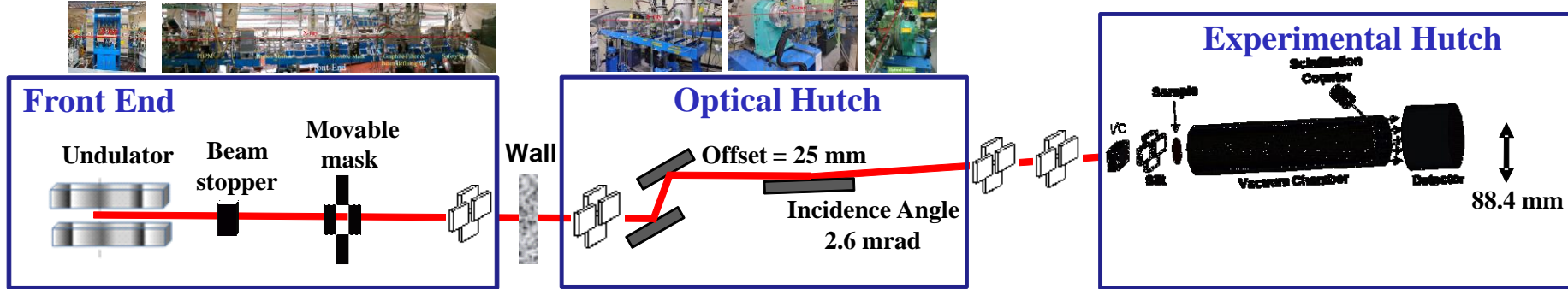


Photograph of optical components in optical hutch and experimental devices in the experimental hutch of the end-station

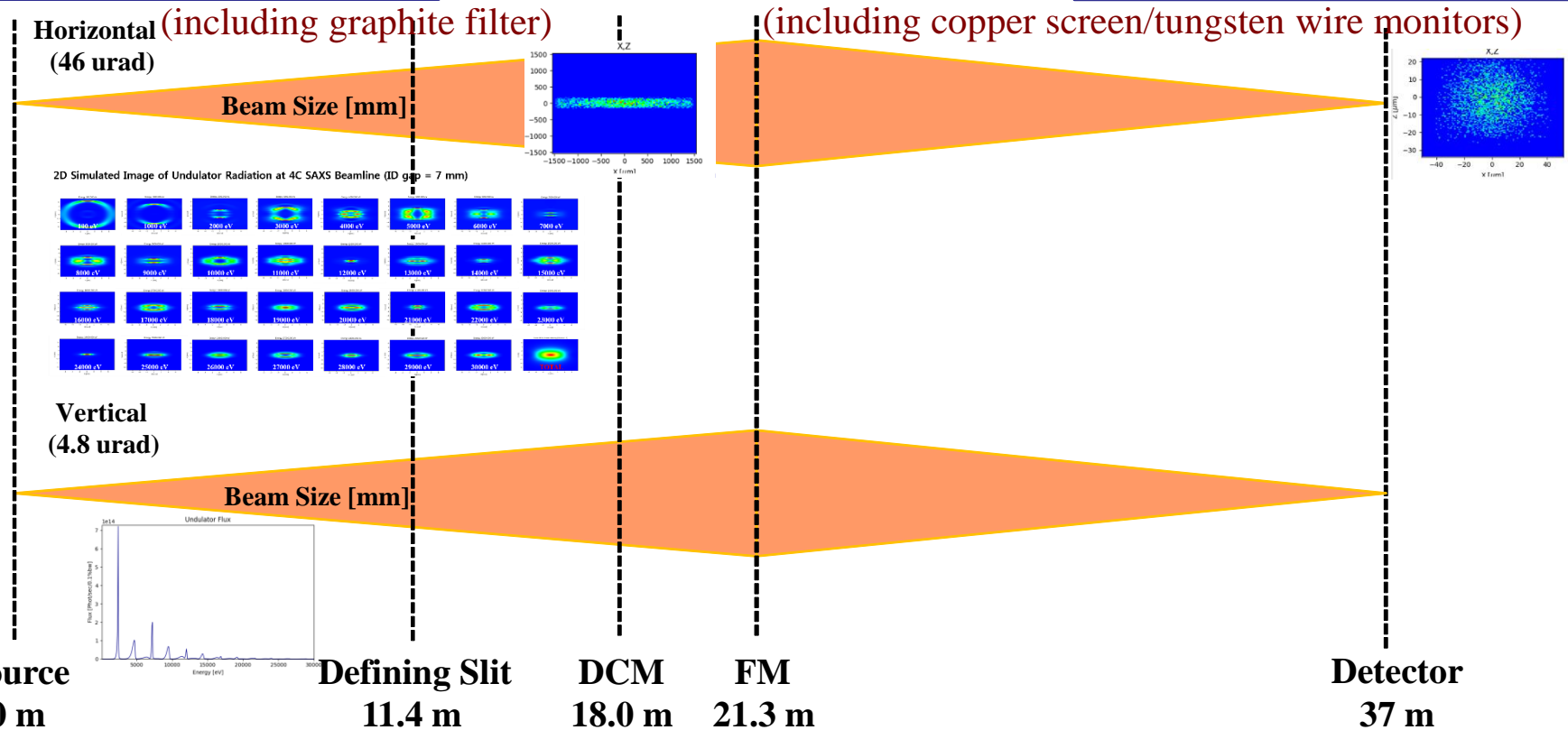
“Small-angle X-ray Scattering Beamline BL4C SAXS at Pohang Light Source II” *Biodesign* 2017, 5 (1), 24-29

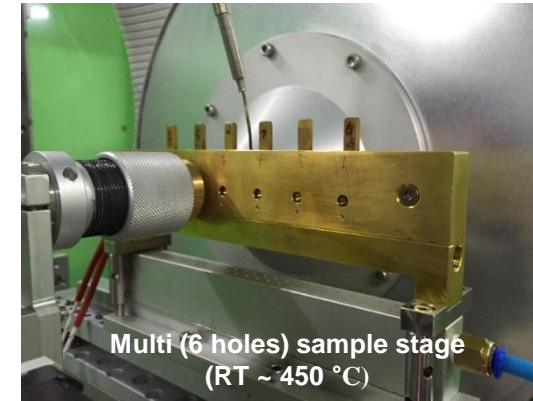
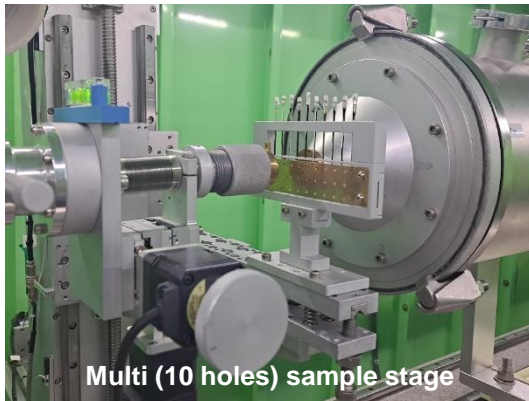
4C SAXS II Beamline Layout

Electron Beam Size = $187 \times 12 \text{ } \mu\text{m}$ (H×V)

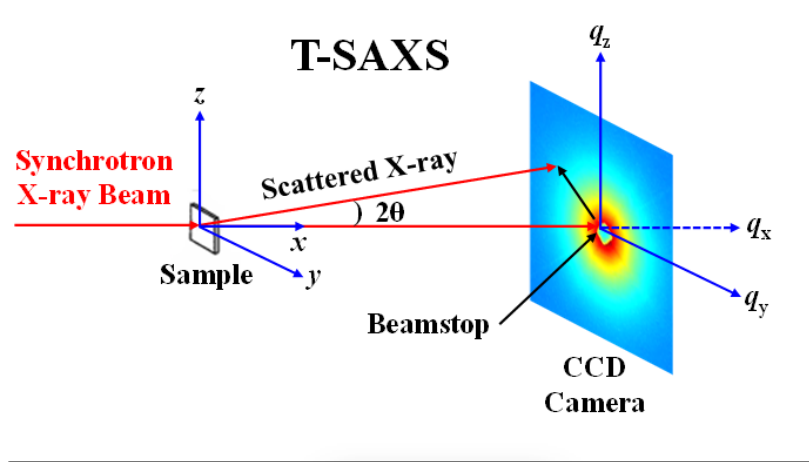
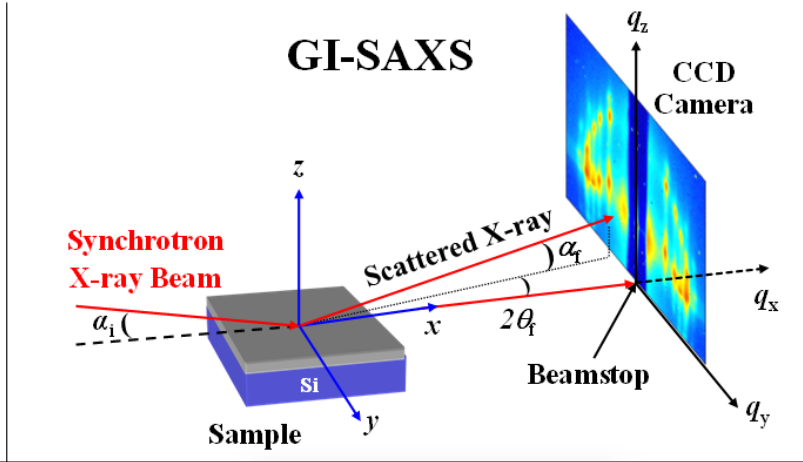
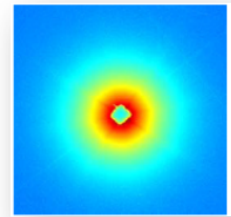
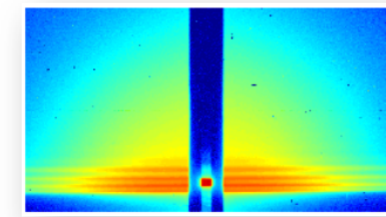


Incident beam height
= 1400 mm

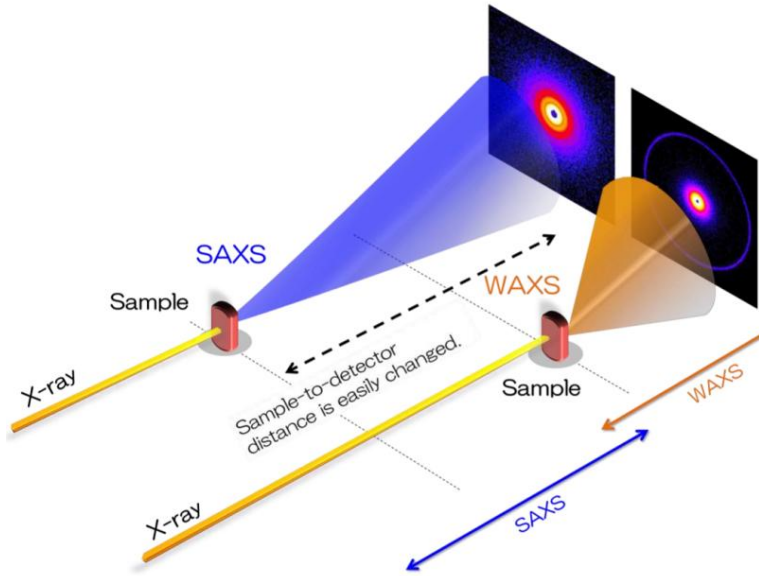




Photograph of experimental sample stages in the experimental hutch of the end-station

<p>T-SAXS</p> 	<p>GI-SAXS</p> 
	
<ul style="list-style-type: none"> Easy measurement Easy analysis In-plane information Bulk samples & Solution samples 	<ul style="list-style-type: none"> Strong intensity Easy preparation of samples In-plane & out-of-plane information ($q_{ }$, q_z) Thin film samples
<ul style="list-style-type: none"> Any possible scattering from substrate Transparency of substrate High energy & High flux X-ray beam 	<ul style="list-style-type: none"> Scattering from surface/internal structure Scattering from reflected & transmitted beam Refraction effects Special setup





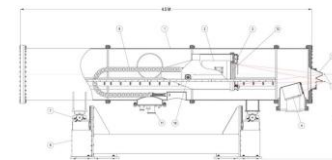
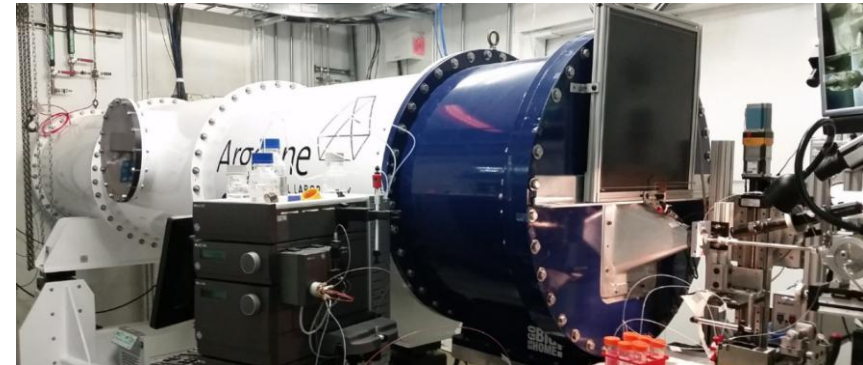
PETRA-III P12 SAXS



PLS-II 4C SAXS

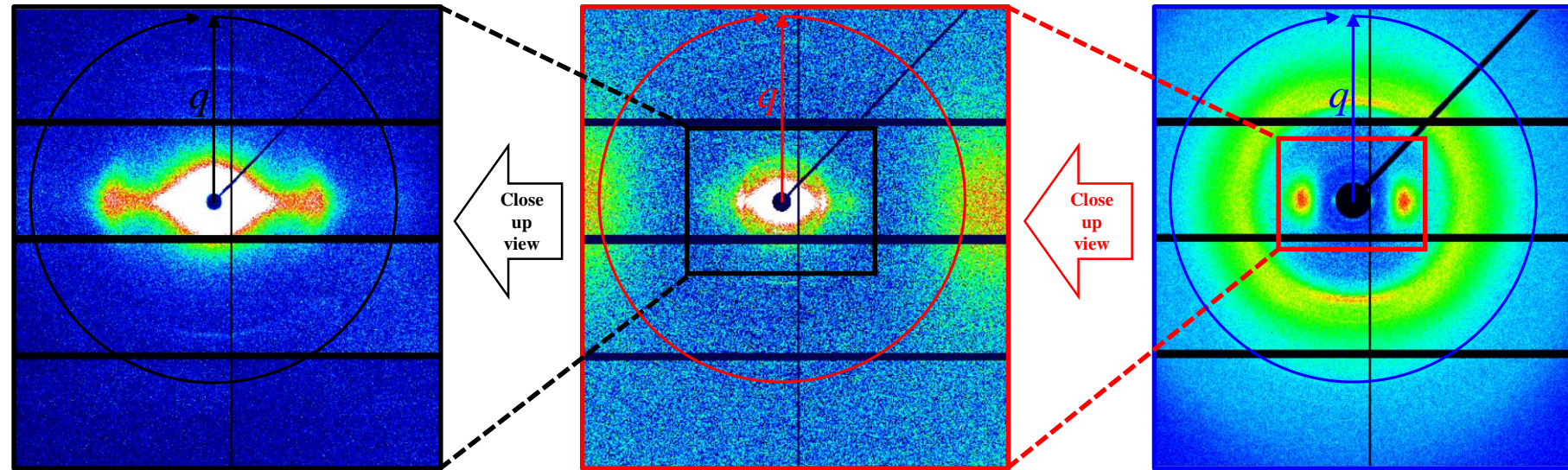
➤ Variable q -range vacuum chamber

- ✓ Facilitate rapid sample-to-detector distance (SDD) change



APS 12 ID-B SAXS

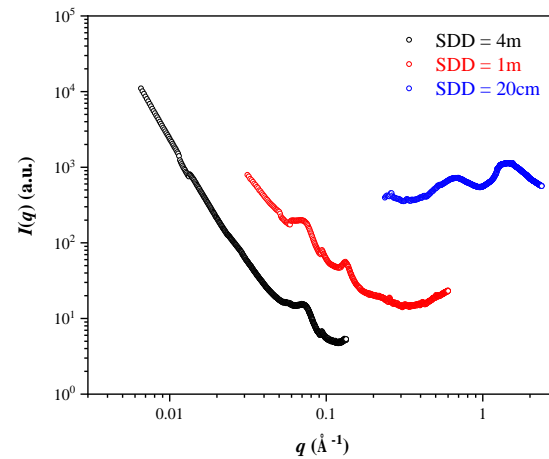
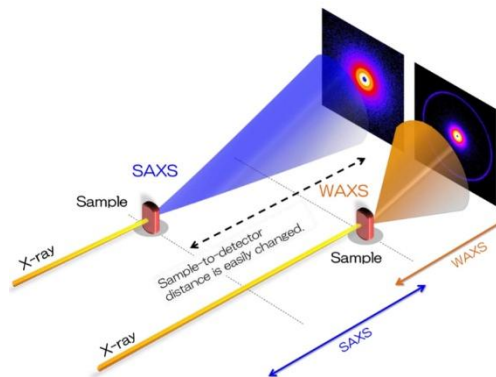
Scattering Patterns of Fiber Strands as a function of SDD

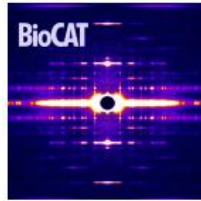


SDD = 4m
($q = 0.0065 \sim 0.1344 \text{ \AA}^{-1}$)

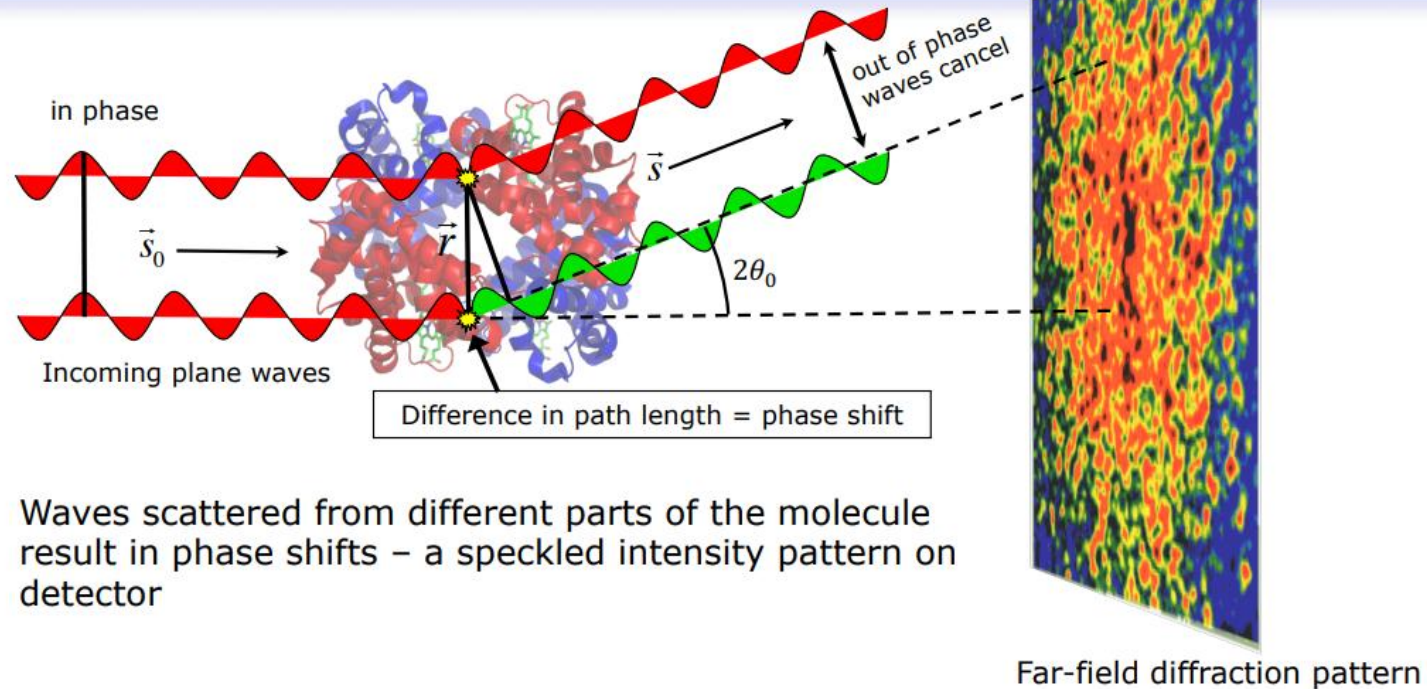
SDD = 1m
($q = 0.0314 \sim 0.6 \text{ \AA}^{-1}$)

SDD = 20cm
($q = 0.237 \sim 2.38 \text{ \AA}^{-1}$)





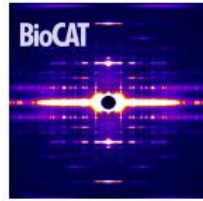
Scattering from a single molecule



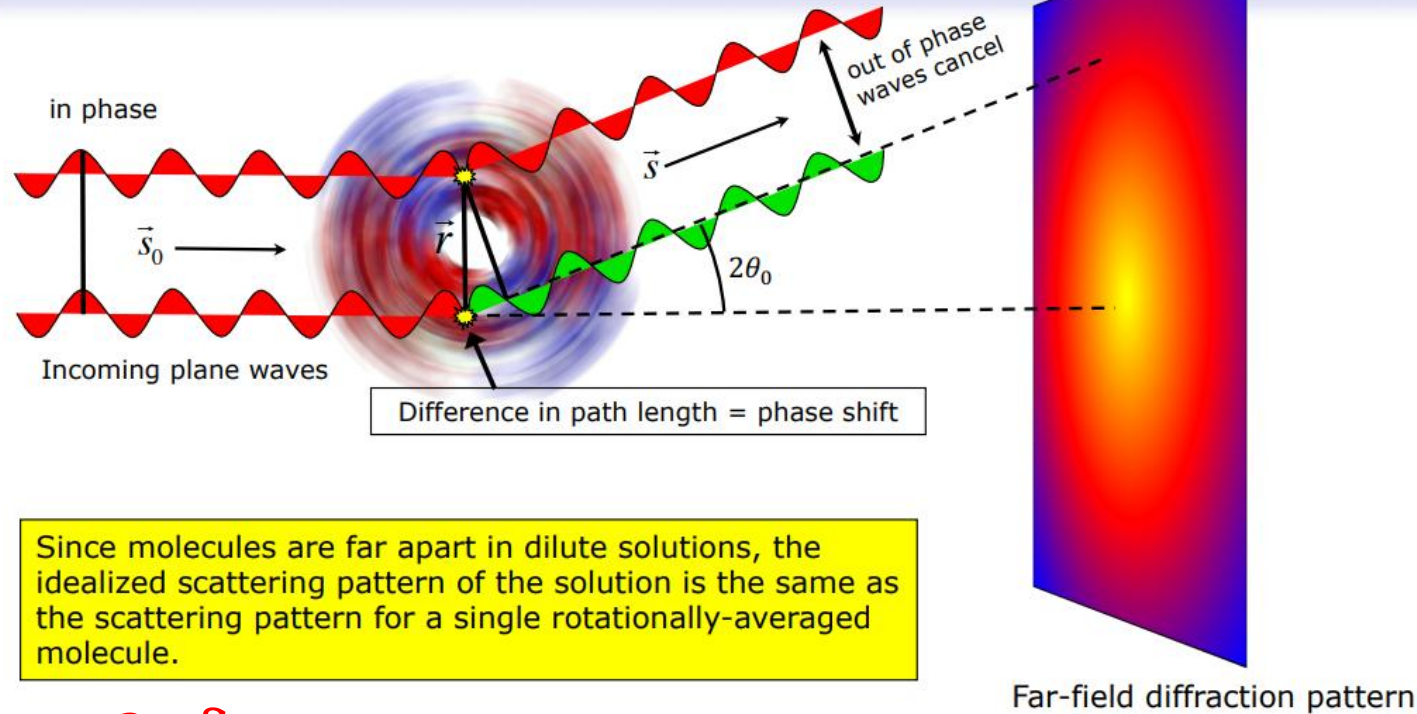
Waves scattered from different parts of the molecule result in phase shifts – a speckled intensity pattern on detector

$$\Delta\phi = \frac{2\pi\delta}{\lambda} \quad A \propto \text{Sum}(A_n, \Delta\phi) \quad I \propto A^2$$

Images from Richard Gillilan's BioSAXS Essentials presentation



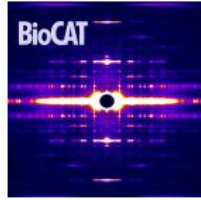
Scattering from molecules in solution



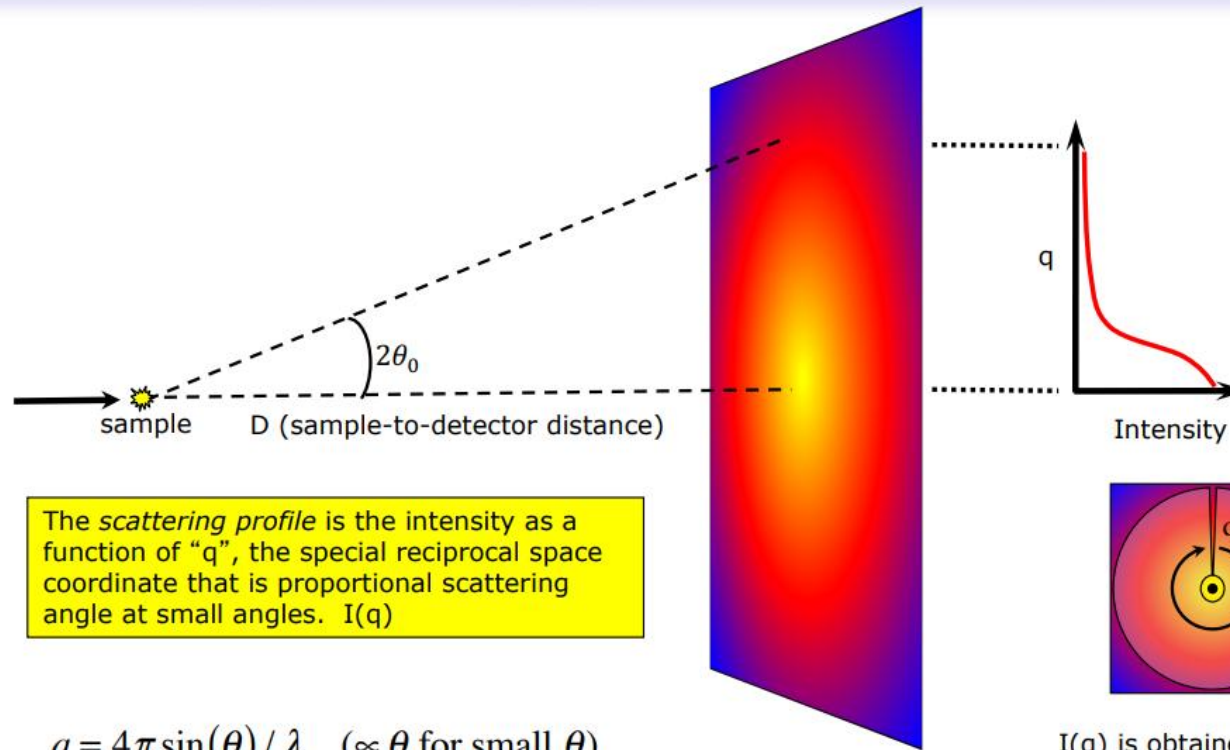
Since molecules are far apart in dilute solutions, the idealized scattering pattern of the solution is the same as the scattering pattern for a single rotationally-averaged molecule.

$$\Delta\phi = \frac{2\pi\delta}{\lambda} \quad A \propto \text{Sum}(A_n, \Delta\phi) \quad I \propto A^2$$

Images from Richard Gillilan's BioSAXS Essentials presentation



The scattering profile



The *scattering profile* is the intensity as a function of “q”, the special reciprocal space coordinate that is proportional scattering angle at small angles. $I(q)$

$$q = 4\pi \sin(\theta) / \lambda \quad (\propto \theta \text{ for small } \theta)$$

$I(q)$ is obtained by integrating around the circle. For detectors, the standard deviation of signal $\sigma(q)$ is also calculated.

Slide from Richard Gillilan’s BioSAXS Essentials presentation

$$I(q) \propto Mc(\rho_1 - \rho_2)^2 |F(q)|^2 S(q)$$

$I(q)$ – Experimental intensity

M – molecular weight

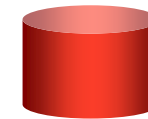
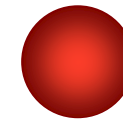
c – concentration

ρ – scattering density (electrons per unit volume)

ρ_1 – particle

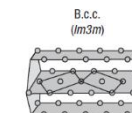
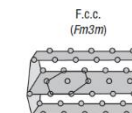
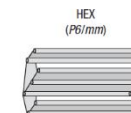
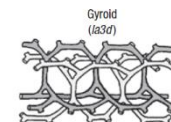
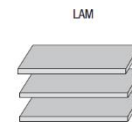
ρ_2 – solvent

$F(q)$ – Form factor, i.e. molecular shape



$S(q)$ – Structure factor, i.e. inter-molecular interaction

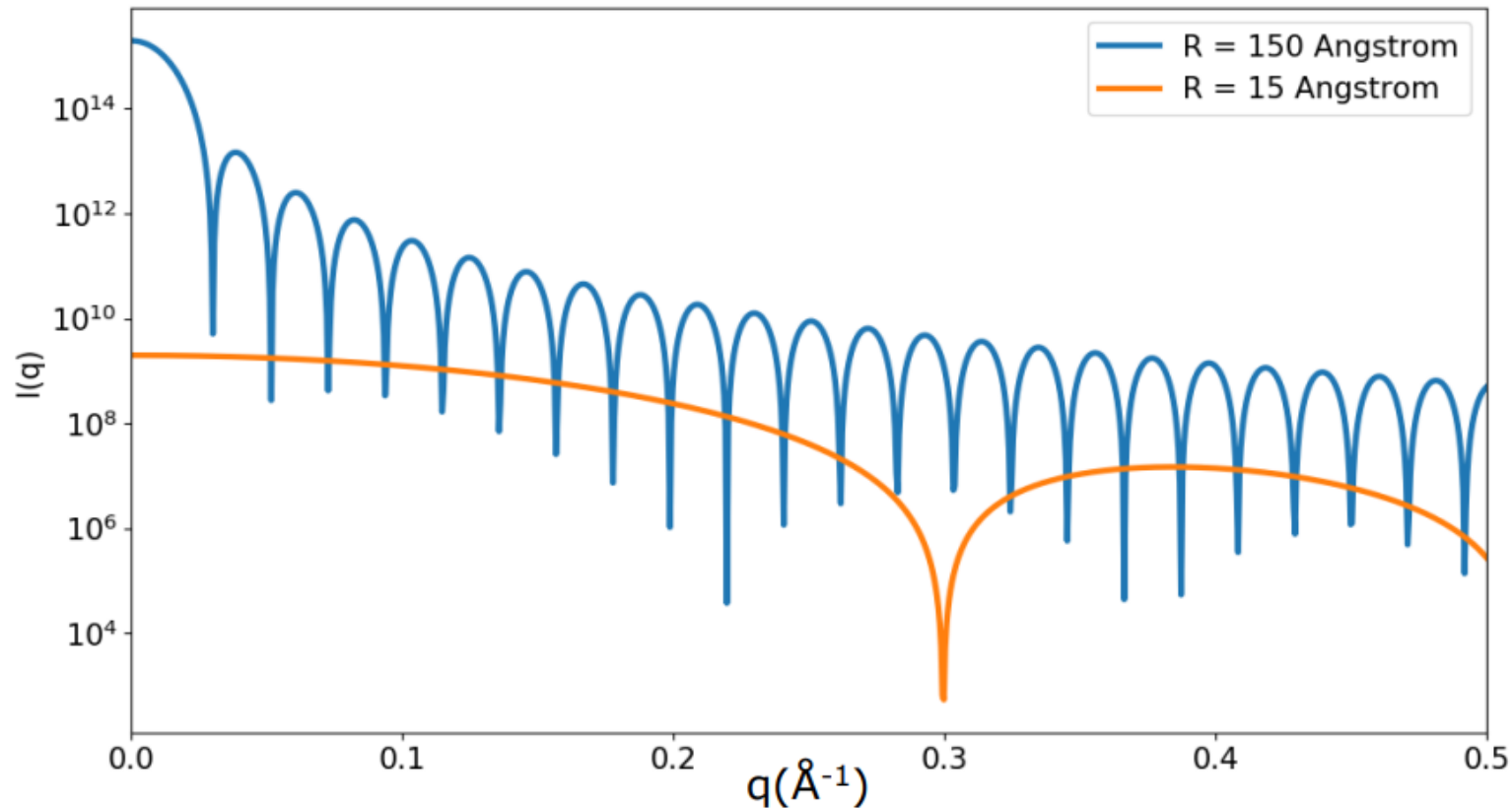
≈ 1 for dilute solutions



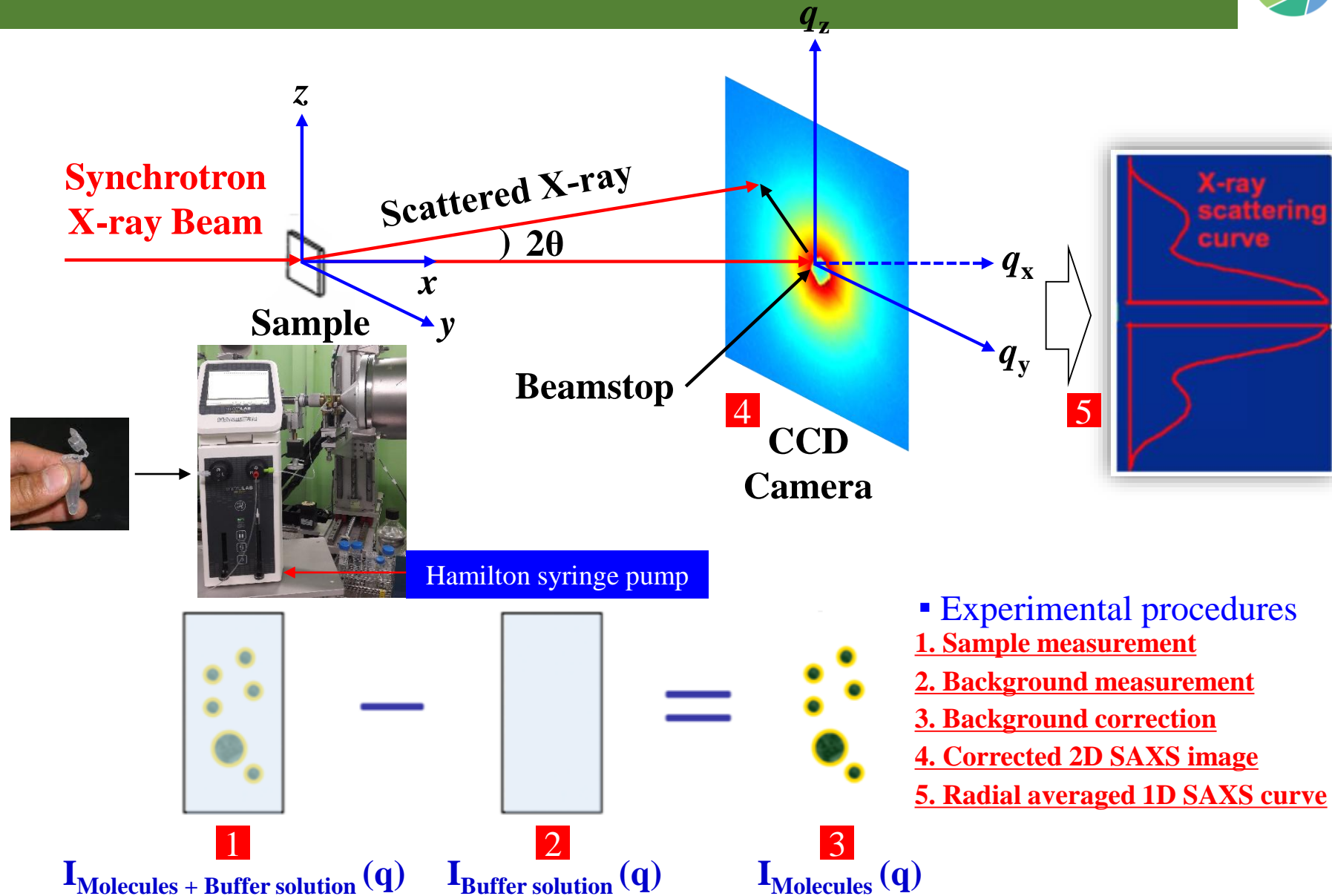
Slide from Jesse Hopkins's BioSAXS Essentials presentation

Scattering from a uniform density sphere with radius R :

$$I(q) \propto \left(\frac{4\pi}{3}R^3\right)^2 \left(3 \frac{\sin(qR) - qR \cos(qR)}{(qR)^3}\right)^2$$

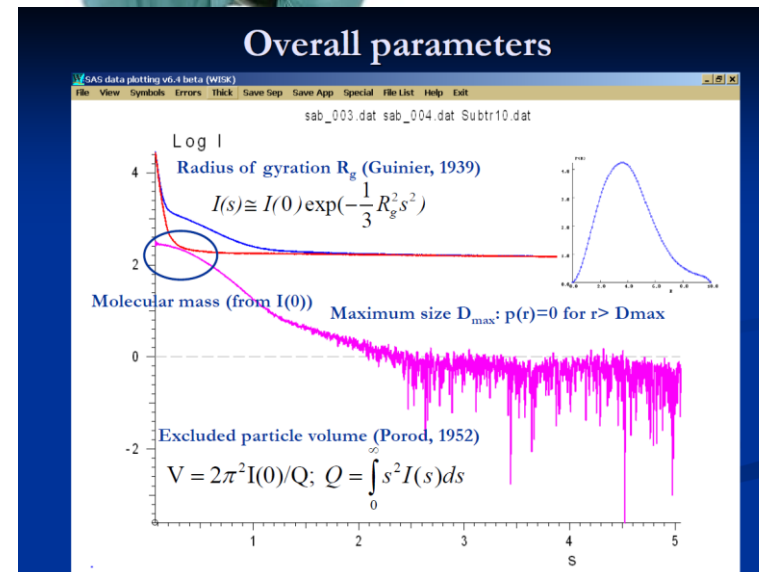


Slide from Jesse Hopkins's BioSAXS Essentials presentation

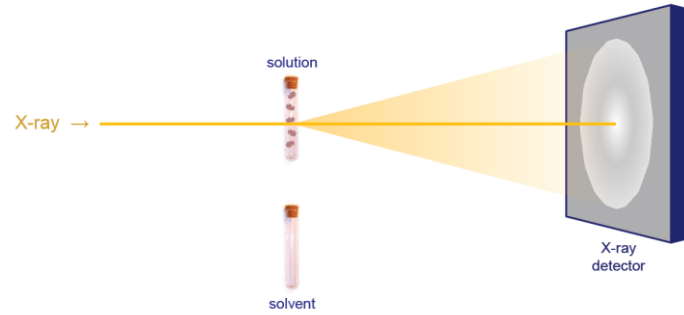


- Experimental procedures
 1. Sample measurement
 2. Background measurement
 3. Background correction
 4. Corrected 2D SAXS image
 5. Radial averaged 1D SAXS curve

- 3D → 2D → 1D
- Experiment design and data reduction
 - Exposure time
 - Background subtraction
 - Dilution series
- Overall parameters:
 - Guinier analysis:
 R_g , $I(0)$, molecular mass
 - Volume
 - $p(r)$, D_{max}

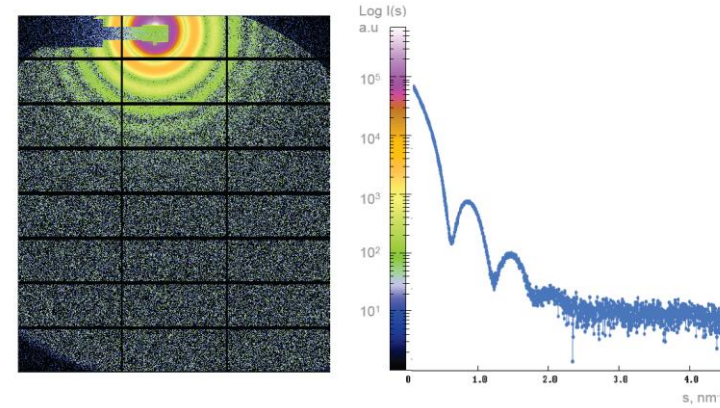


SAXS experiment

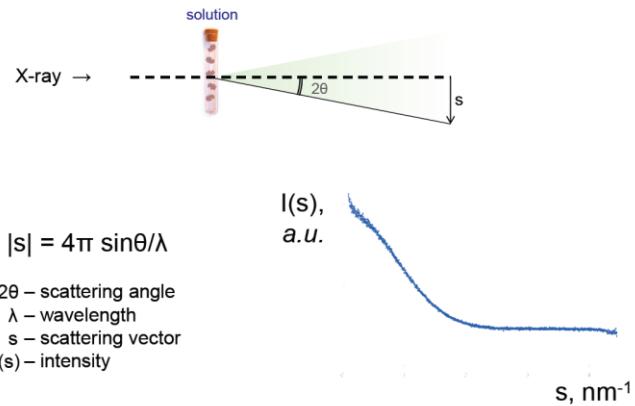


- Few kDa to GDa
- Monodisperse and homogeneous
- Concentration: 0.5–10 mg/ml
- Amount: 10–100 μ l

2D \rightarrow 1D



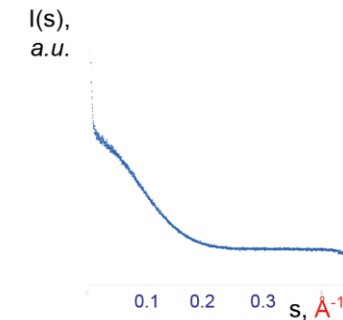
Notations and units



Notations and units

$$|s| = 4\pi \sin\theta/\lambda$$

2θ – scattering angle
 λ – wavelength



X-rays - Radiation damage!!!

- With intense synchrotron beam: radiation damage:

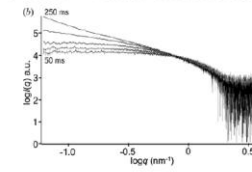


Free radicals: oxidize proteins which leads to their aggregation

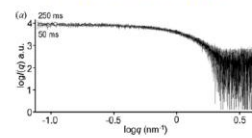
- Monitor radiation damage: collect several frames and compare them.
- Limit the radiation damage

X-rays - Radiation damage!!!

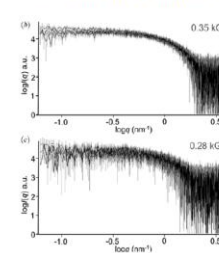
Rnase – Static measurement



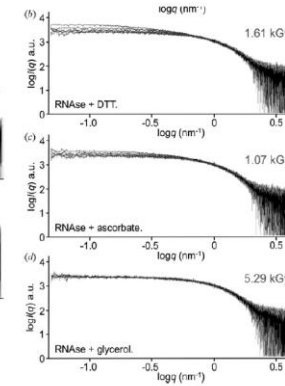
Flow measurement

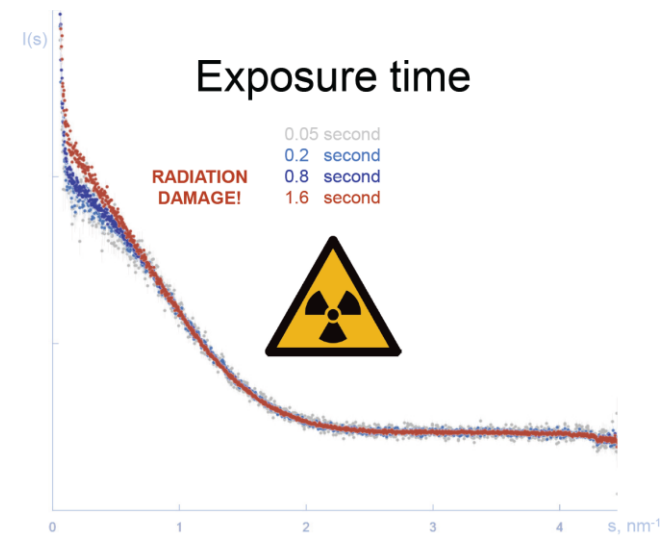
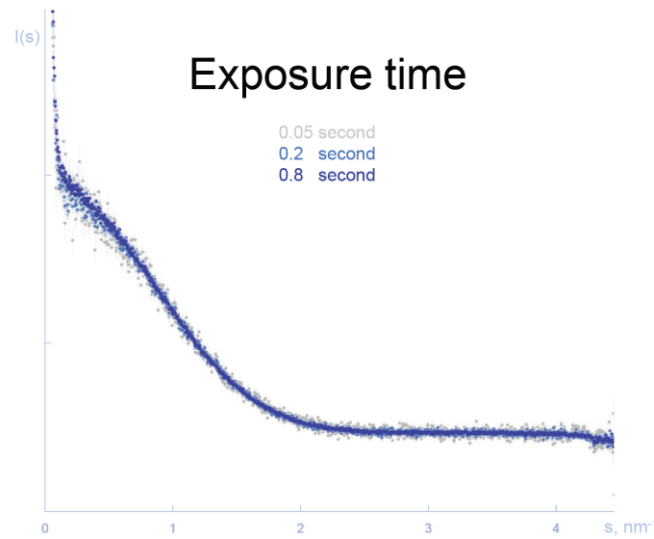
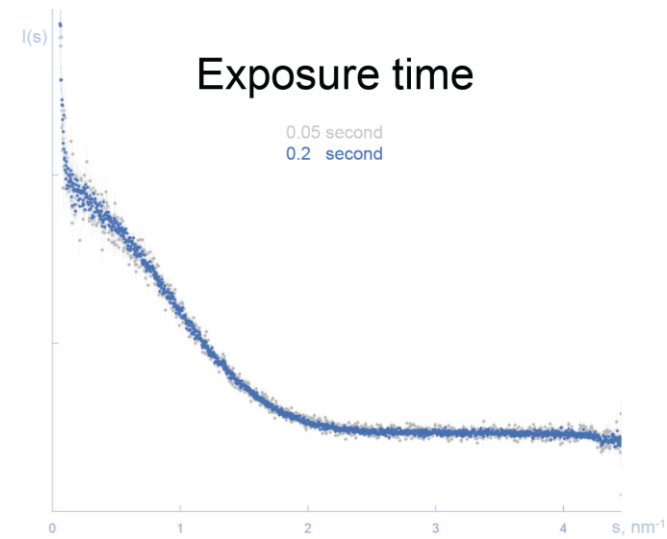
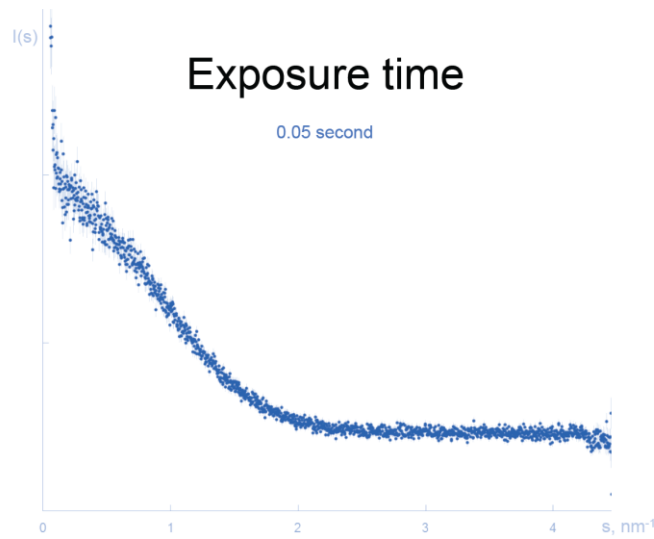


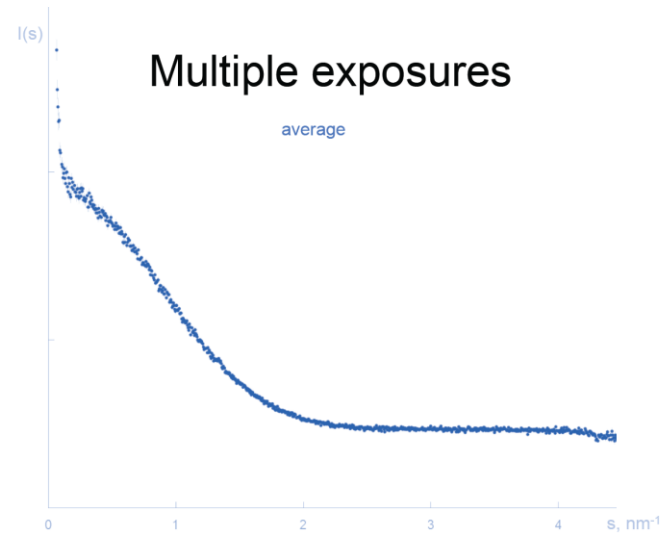
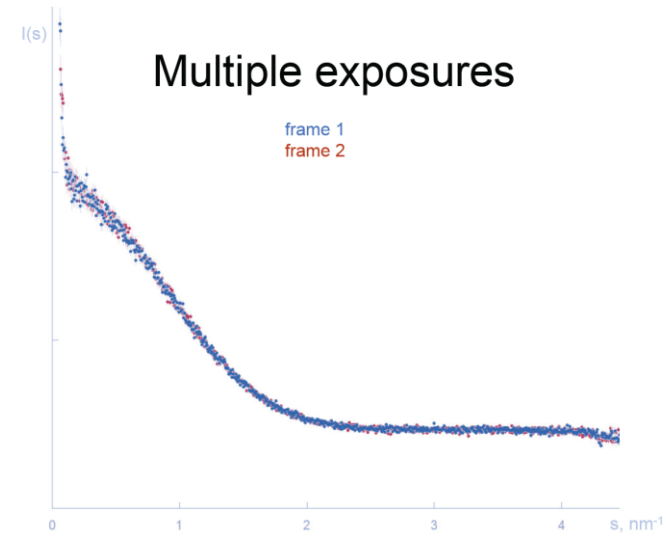
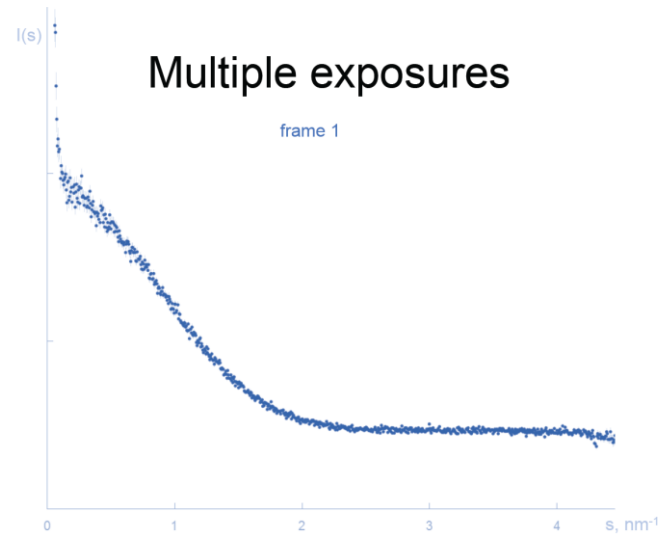
Beam attenuation



Use of additives

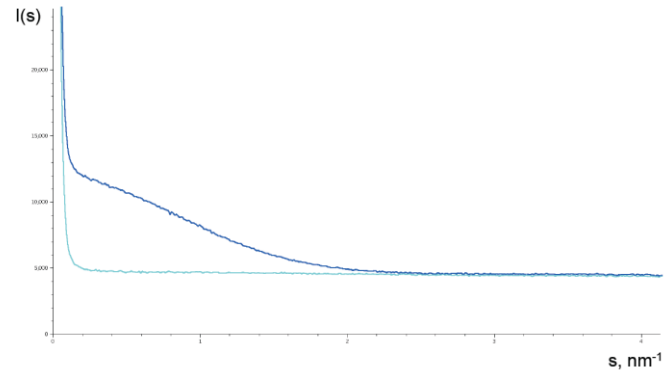






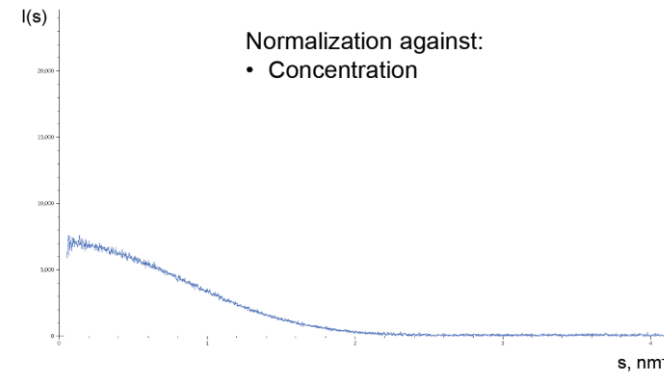
Background subtraction

Solution minus Solvent

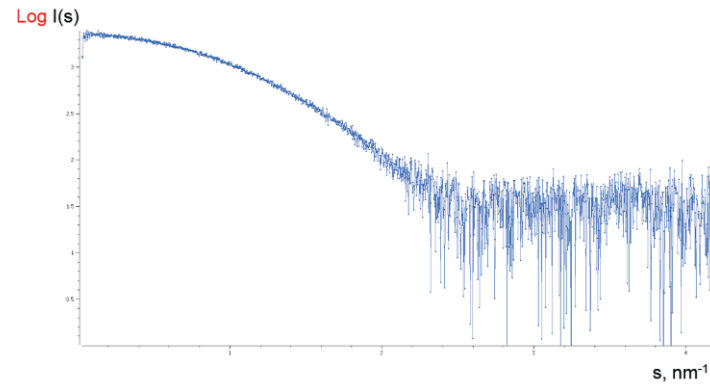


Background subtraction

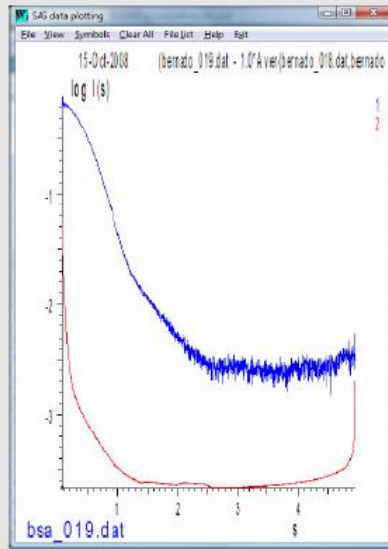
Solution minus Solvent



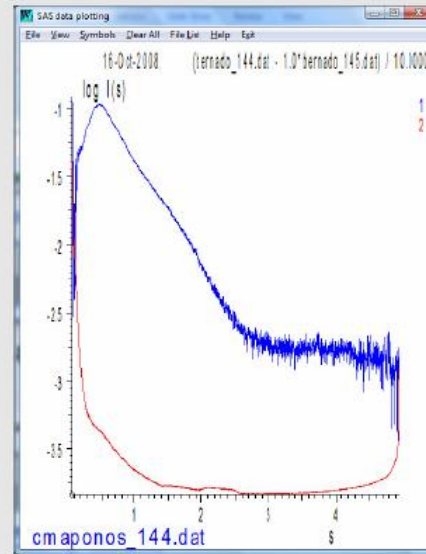
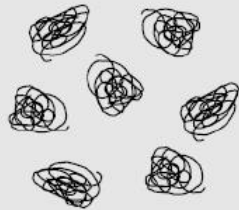
Logarithmic plot



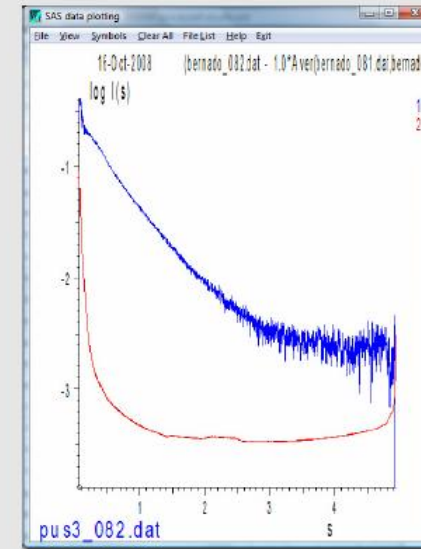
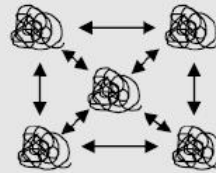
Inter-particle interactions



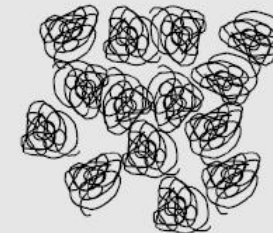
Ideal solution of particles



Repulsive particle interactions



Attractive particle interactions



Radius of gyration (R_g)

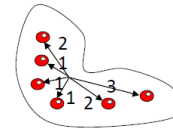
Definition

Measure for the overall size of a macromolecule

Average of square center-of-mass distances in the molecule weighted by the scattering length density

R_g^2 is the average electron density weighted squared distance of the scatters from the centre of the object

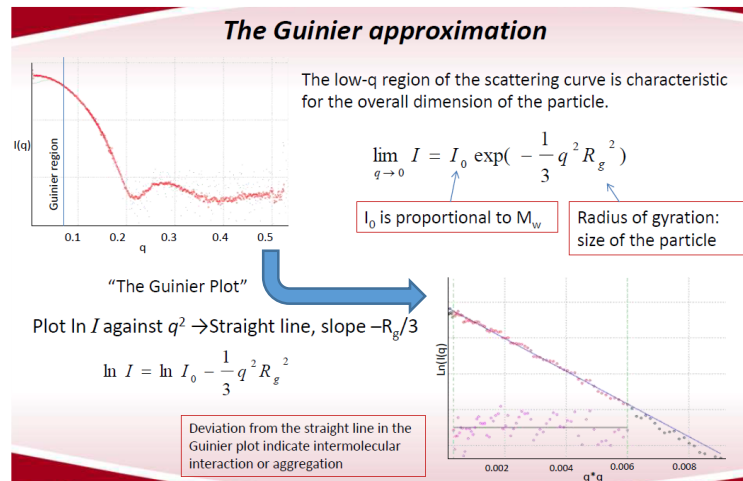
$$R_g^2 = \frac{\int \mathbf{r}^2 \rho(\mathbf{r}) d\mathbf{r}}{\int \rho(\mathbf{r}) d\mathbf{r}}$$



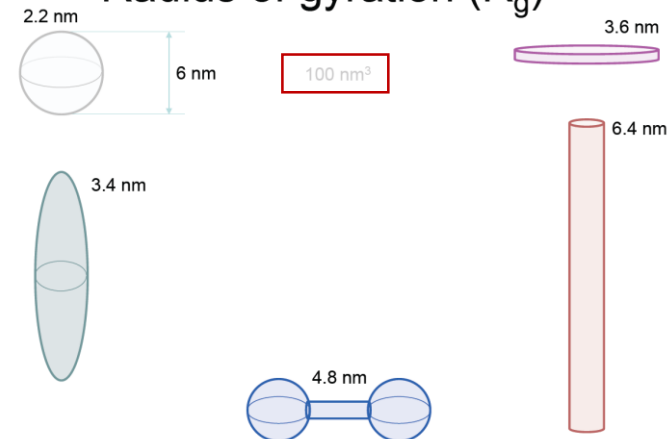
$$R_g^2 = (1^2 + 1^2 + 1^2 + 2^2 + 2^2 + 3^2) / 6 = 20/6$$

$$R_g = \sqrt{3.333} = 1.82$$

- Solid sphere radius R:
 $R_g = \sqrt{3/5} R$
- Thin rod length L
 $R_g = \sqrt{1/12} L$
- Thin disk radius R:
 $R_g = \sqrt{1/2} R$



Radius of gyration (R_g)



Aggregation



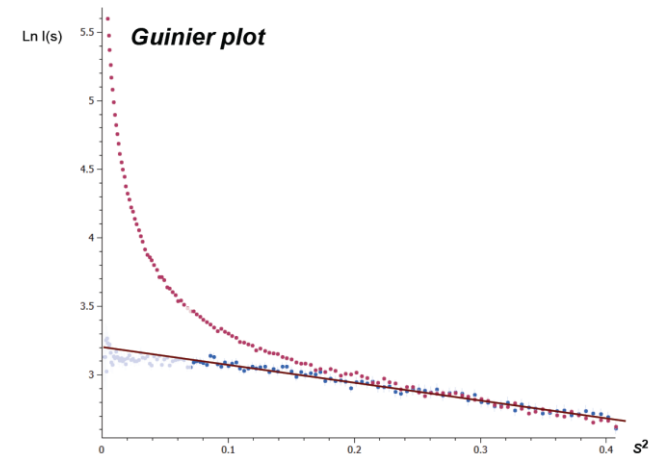
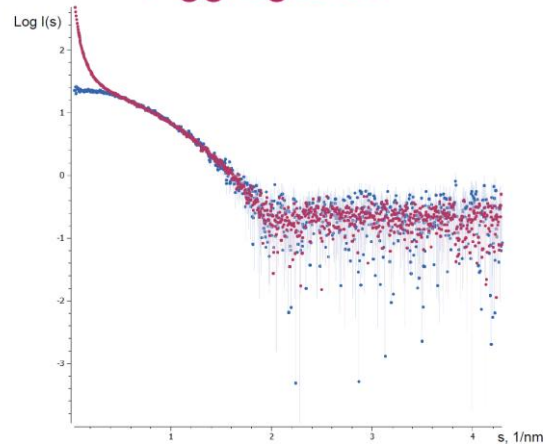
Monodisperse sample

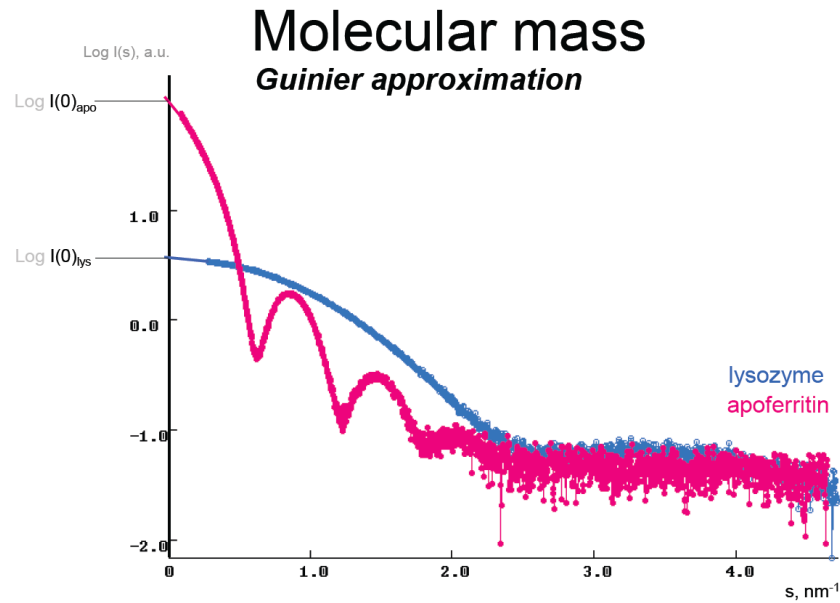
Aggregation



Aggregated sample

Aggregation





$I(0)$ and Molecular Mass

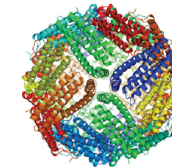
$$\frac{MM_{\text{sample}}}{MM_{\text{BSA}}} = \frac{I(0)_{\text{sample}}}{I(0)_{\text{BSA}}}$$

$$MM_{\text{sample}} = I(0)_{\text{sample}} \cdot MM_{\text{BSA}} / I(0)_{\text{BSA}}$$

BSA $R_g = 3.1$ nm
 $I(0) = 11.7$ a.u.
 $MM_{\text{BSA}} = 66$ kDa



$R_g = 1.46$ nm
 $I(0) = 2.68$ a.u.
 $MM = 15.1$ kDa



$R_g = 6.81$ nm
 $I(0) = 79.45$ a.u.
 $MM = 450$ kDa

Porod volume

Excluded volume of the hydrated particle

$$V_P = \frac{2\pi^2 I(0)}{\int_0^\infty [I(s) - K_4] s^2 ds}$$

K_4 is a constant determined to ensure the asymptotical intensity decay proportional to s^{-4} at higher angles following the Porod's law for homogeneous particles

Porod law

Excluded volume of the hydrated particle



21 nm³

~13 kDa

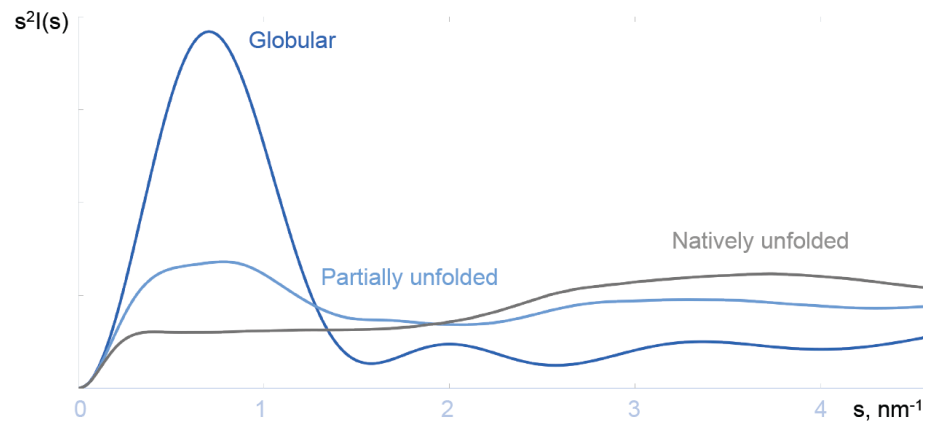


974 nm³

~610 kDa

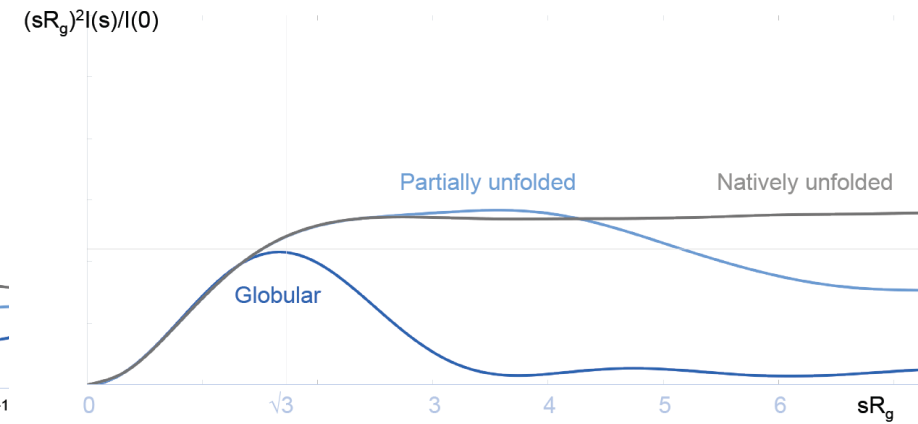
Kratky plot

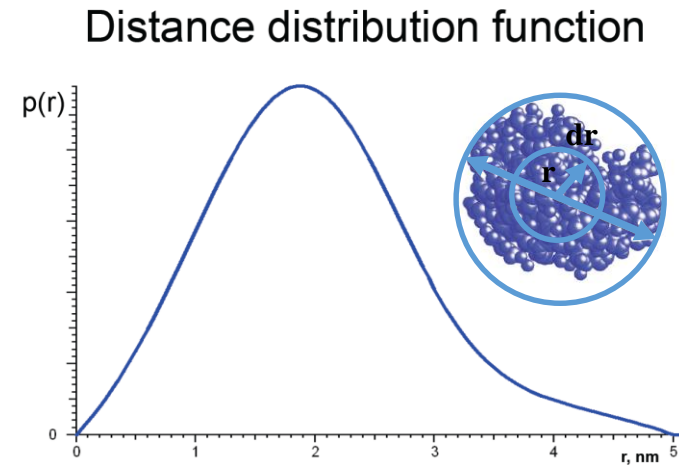
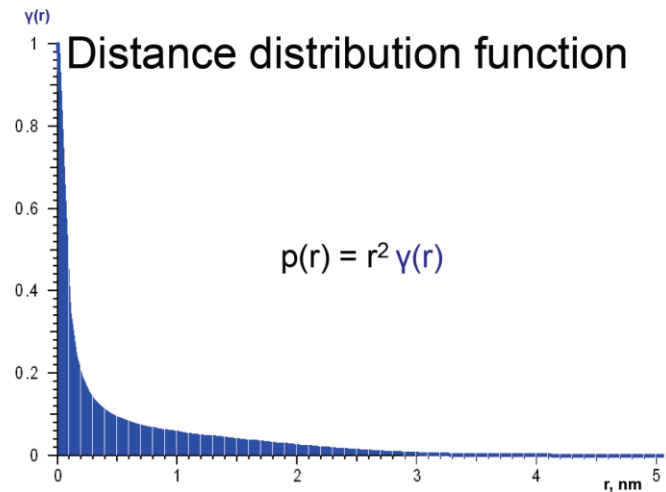
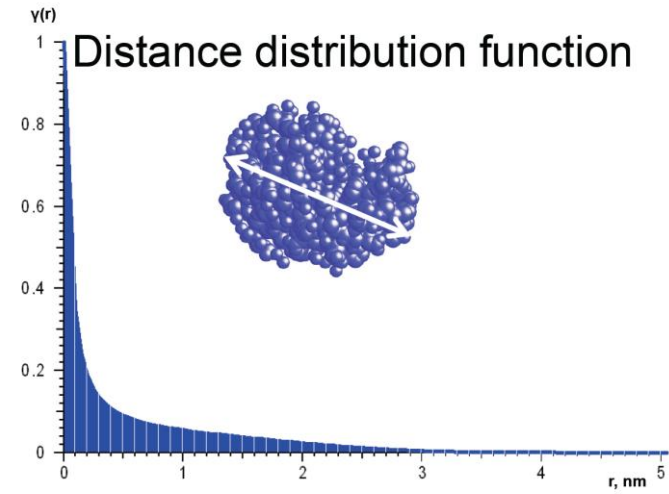
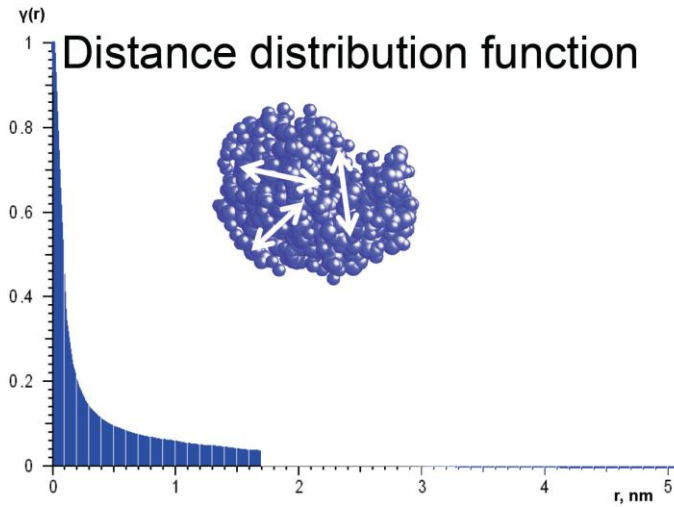
Patterns of globular and flexible proteins



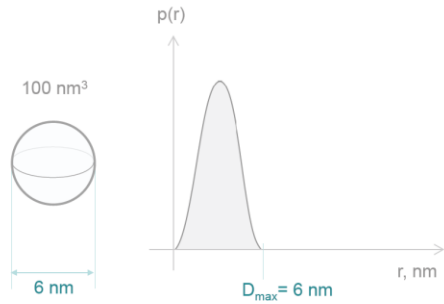
Normalized Kratky plot

Patterns of globular and flexible proteins

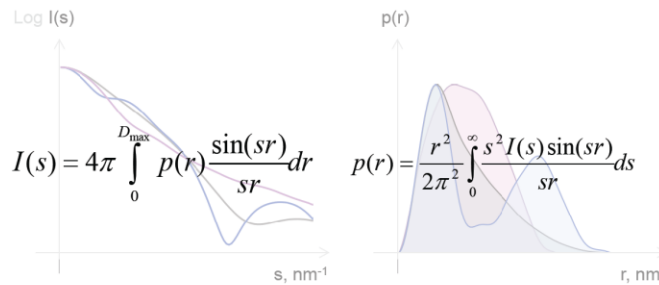
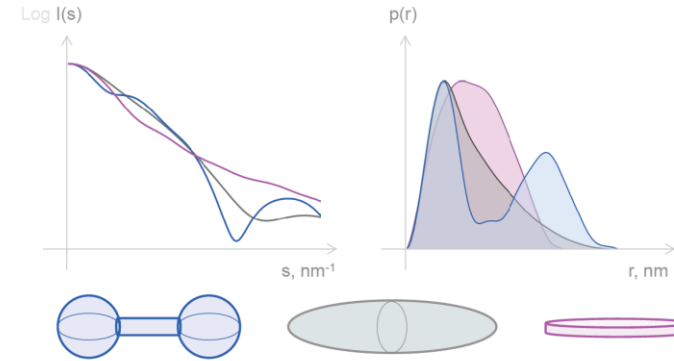




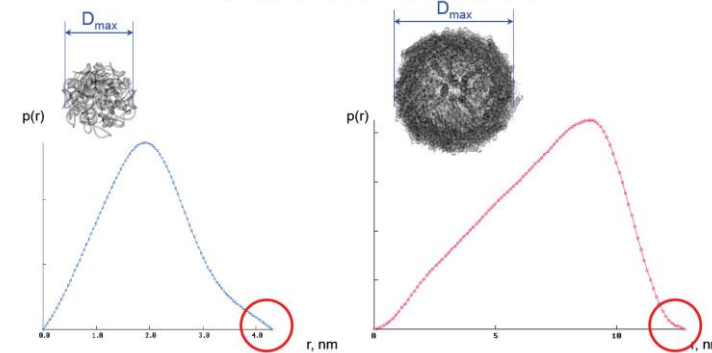
Distance distribution function



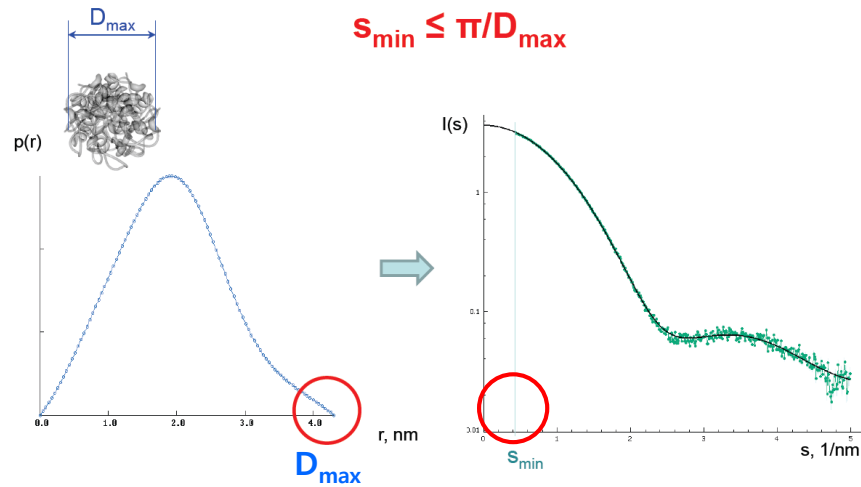
Distance distribution function



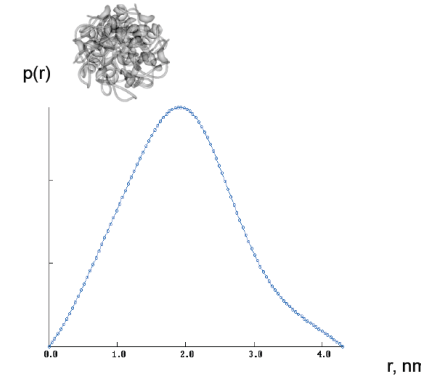
$p(r)$ plot Distance distribution function



Data quality



R_g and $I(0)$ from $p(r)$



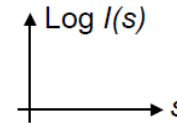
$$I(0) = 4\pi \int_0^{D_{\max}} p(r) dr$$

$$R_g^2 = \frac{\int_0^{D_{\max}} r^2 p(r) dr}{2 \int_0^{D_{\max}} p(r) dr}$$

Summary

- Exposure 3D → 2D
- Radial averaging → 1D
- Normalization
- Background subtraction
- Analysis

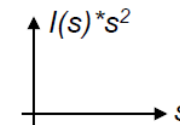
- Log plot



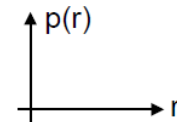
- Guinier plot (R_g , MM)



- Kratky plot (flexibility)



- $p(r)$ plot



1. Model Independent Approach: Ab initio methods

- *Monodisperse* systems (size, shape)
- Biomacromolecules (Protein, DNA, RNA) and Self-assembled Nanoparticles

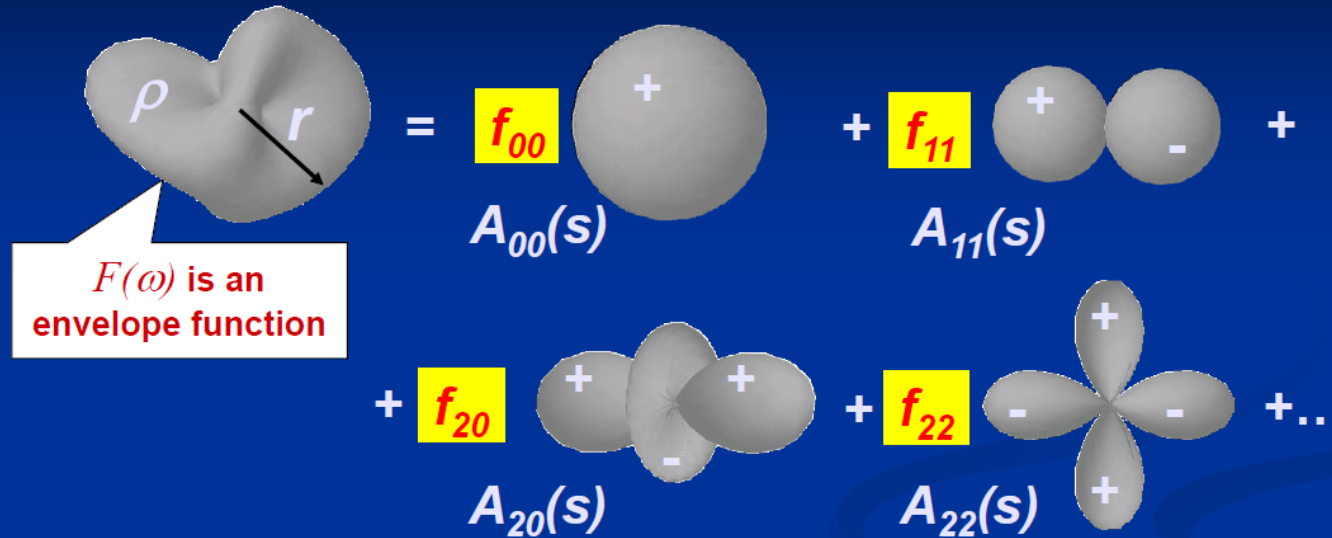
2. Model Dependent Approach: Scatter, SASfit, SASView, etc.

- Monodisperse and *polydisperse* systems (size)
- Self-assembled Nanoparticles

1.1. Model Independent Approach: Ab initio methods

Shape parameterization by spherical harmonics

Homogeneous particle



$F(\omega)$ is an envelope function

$$F(\omega) = f_{00} A_{00}(s) + f_{11} A_{11}(s) + f_{20} A_{20}(s) + f_{22} A_{22}(s) + \dots$$

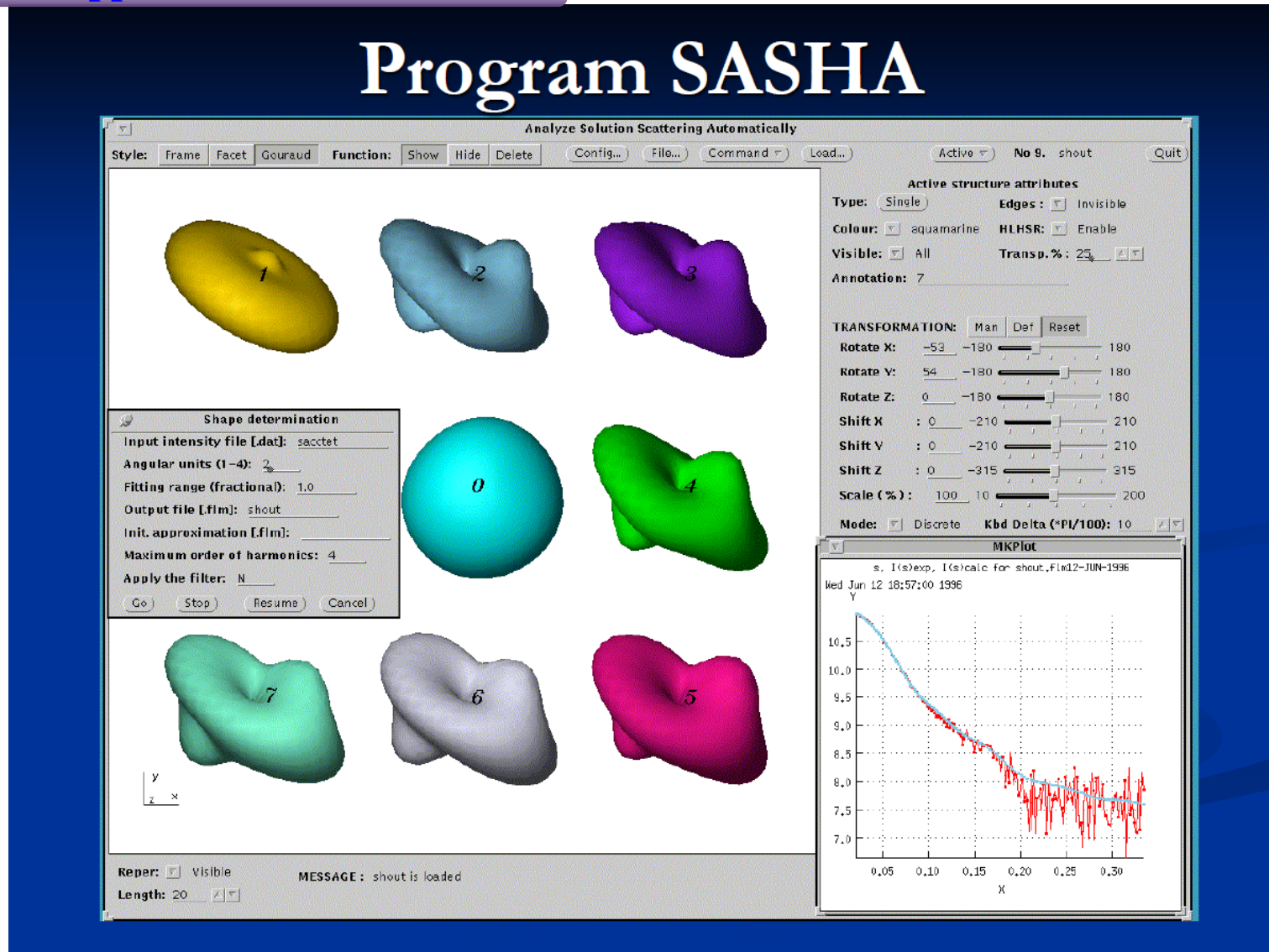
Spatial resolution:

$$\delta = \frac{\pi R}{L+1}, \quad R - \text{radius of an equivalent sphere.}$$

Number of model parameters f_{lm} is $(L+1)^2$.

One can easily impose symmetry by selecting appropriate harmonics in the sum. This significantly reduces the number of parameters describing $F(\omega)$ for a given L .

1.2. Model Independent Approach: Ab initio methods

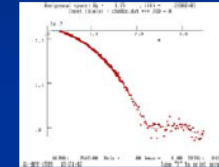


1.3. Model Independent Approach: Ab initio methods

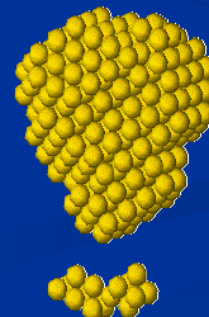
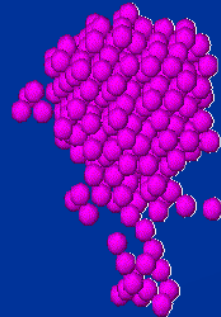
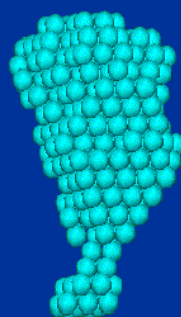
Ab initio program DAMMIN

Using simulated annealing, finds a compact dummy atoms configuration X that fits the scattering data by minimizing

$$f(X) = \chi^2 [I_{\text{exp}}(s), I(s, X)] + \alpha P(X)$$



where χ is the discrepancy between the experimental and calculated curves, $P(X)$ is the penalty to ensure compactness and connectivity, $\alpha > 0$ its weight.



compact

loose

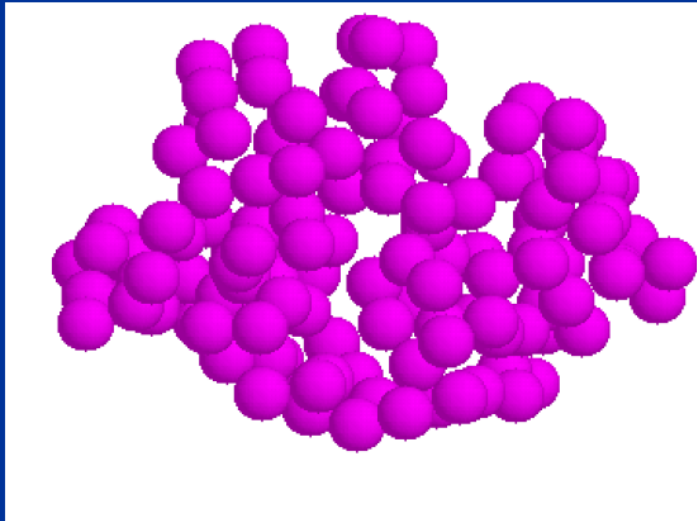
disconnected

1.4. Model Independent Approach: Ab initio methods

Ab initio dummy residues model

- Proteins typically consist of folded polypeptide chains composed of amino acid residues

At a resolution of 0.5 nm a protein can be represented by an ensemble of K dummy residues centered at the $C\alpha$ positions with coordinates $\{r_i\}$



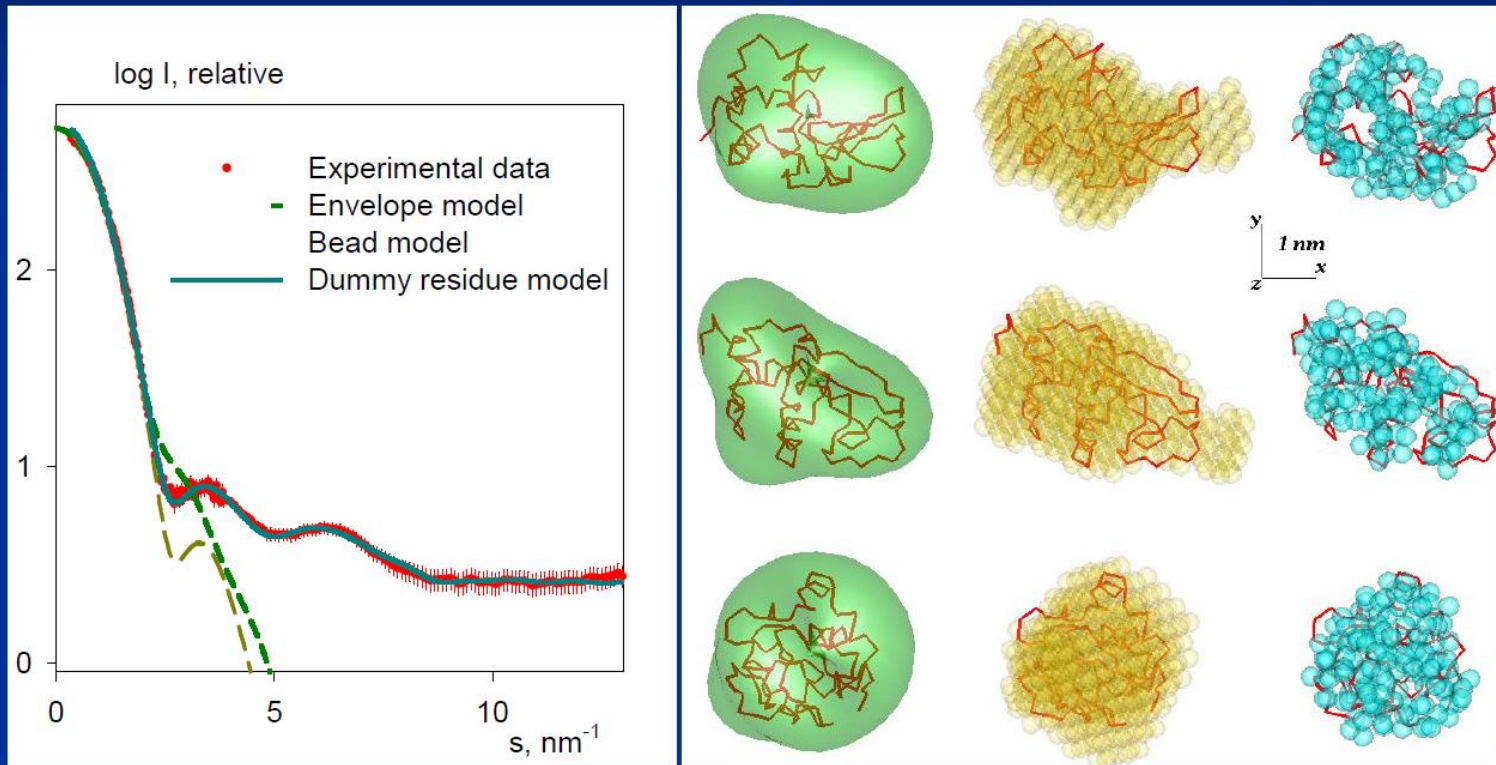
Scattering from such a model is computed using the Debye (1915) formula.

Starting from a random model, simulated annealing is employed similar to DAMMIN

1.5. Model Independent Approach: Ab initio methods

Benchmarking *ab initio* methods

Envelope *Bead model* *Dummy residues*



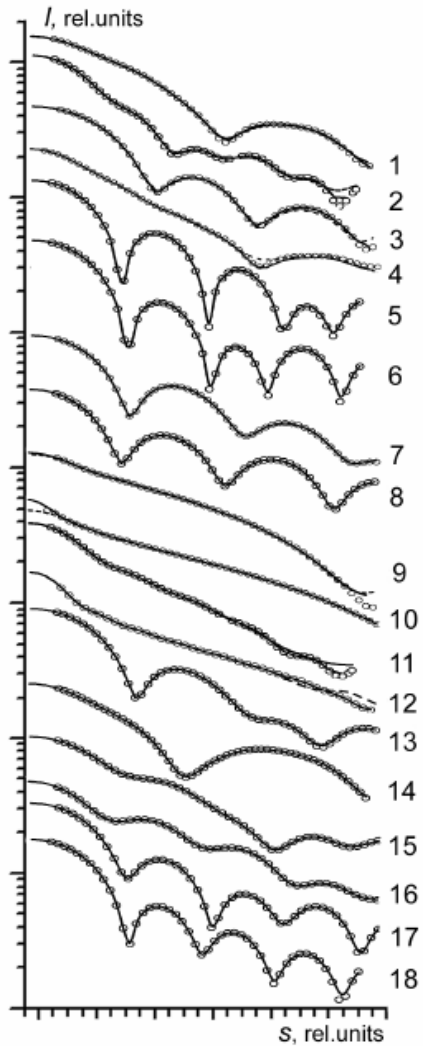
Comparison with the crystal structure of lysozyme

**SASHA
1996**

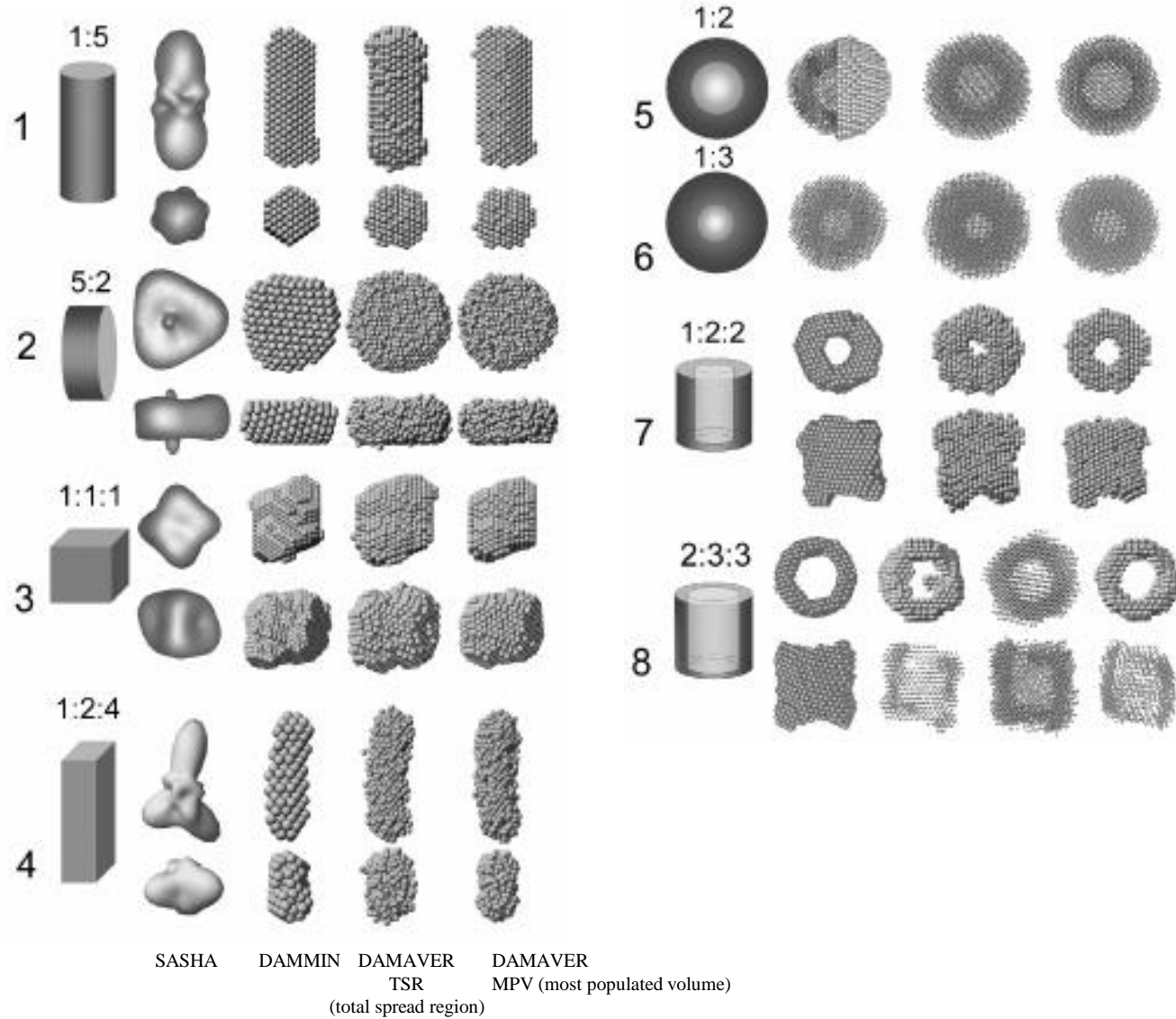
**DAMMIN
1999**

**GASBOR
2001**

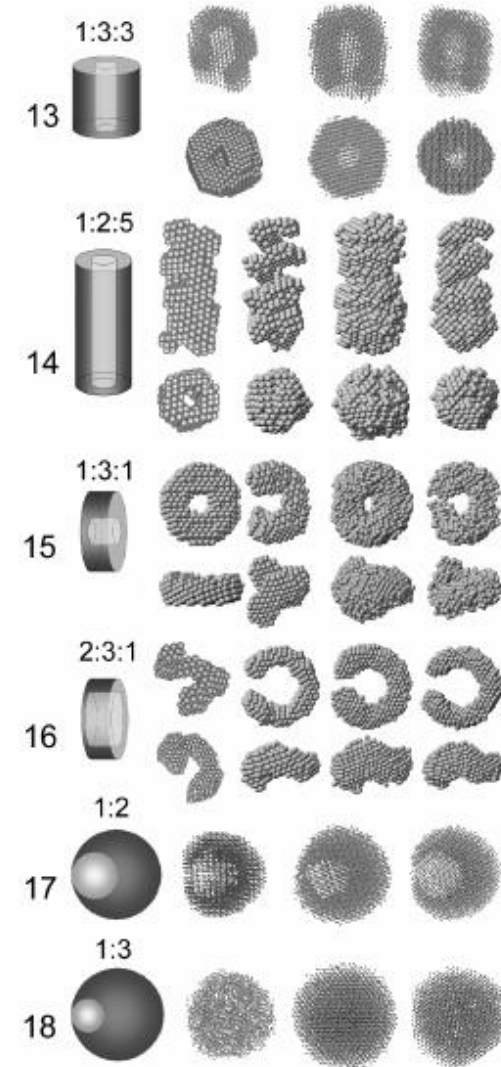
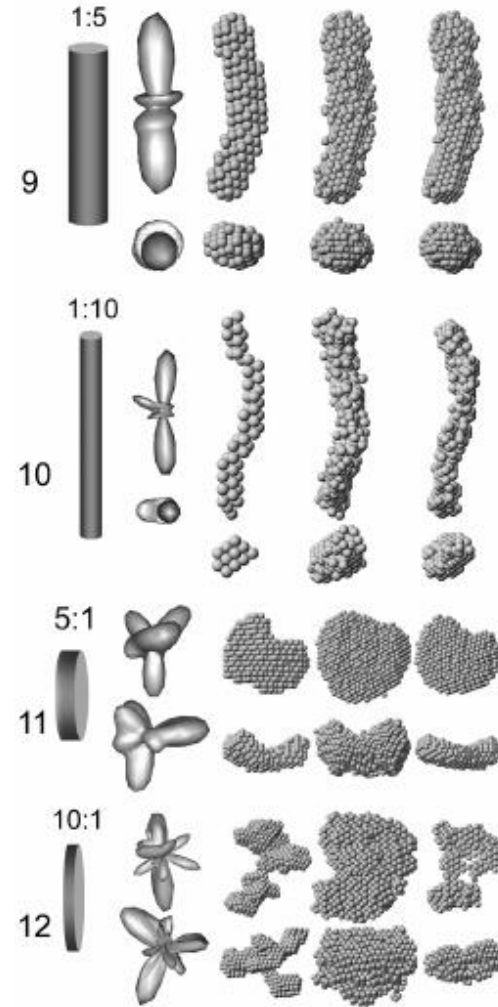
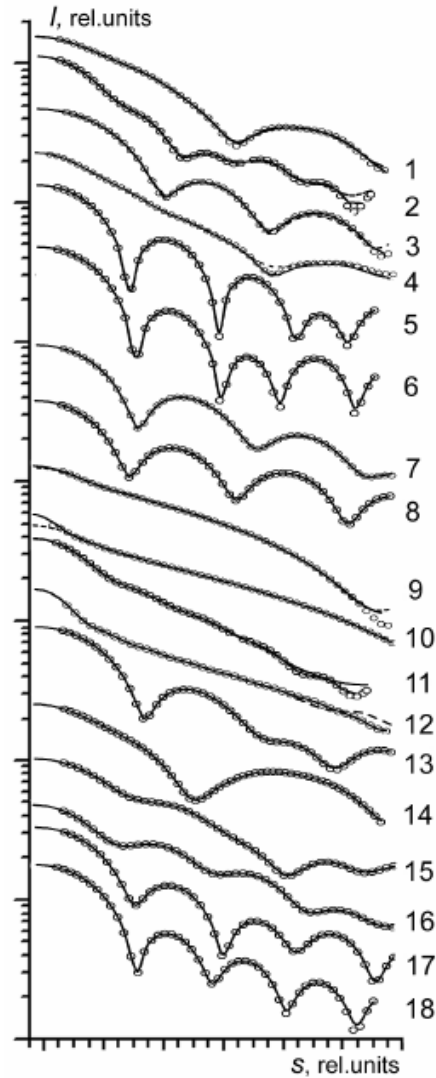
1.6. Model Independent Approach: Ab initio methods



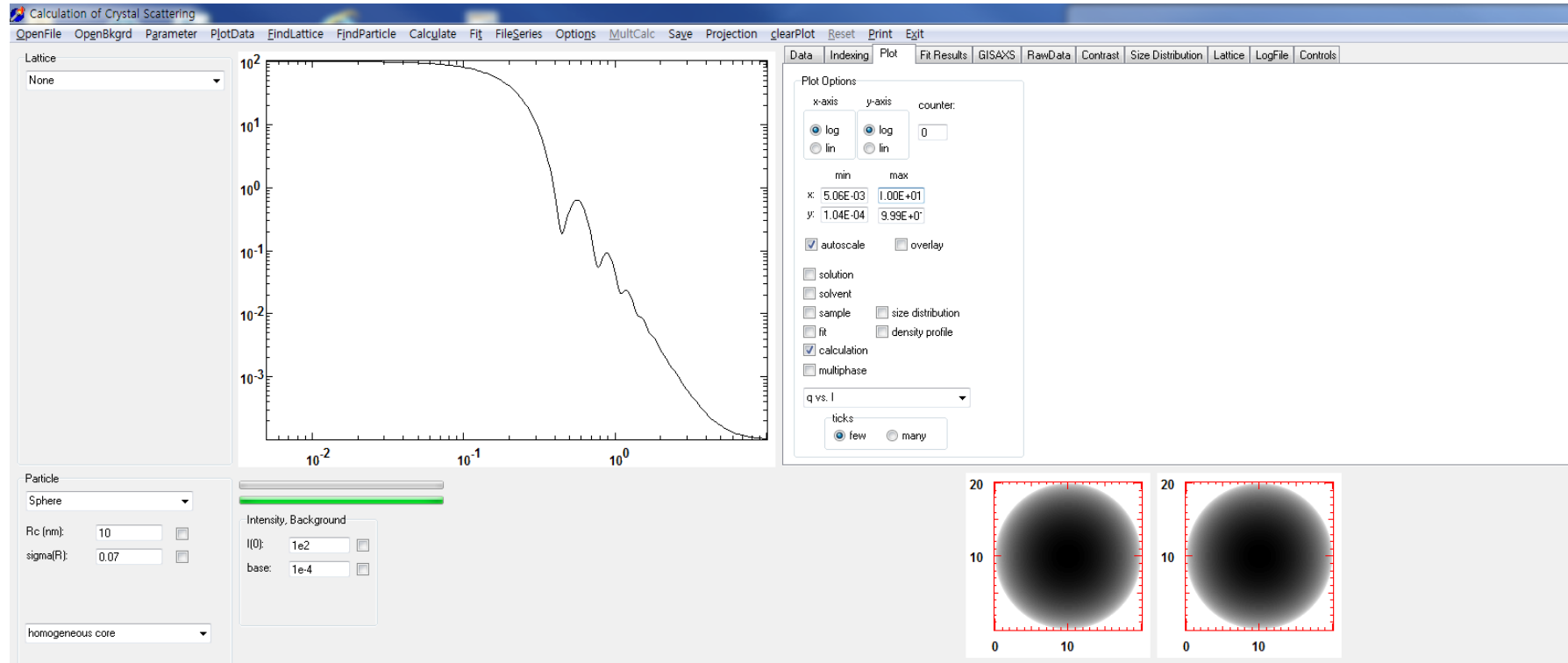
J. Appl. Cryst. 2003. 36, 860-864



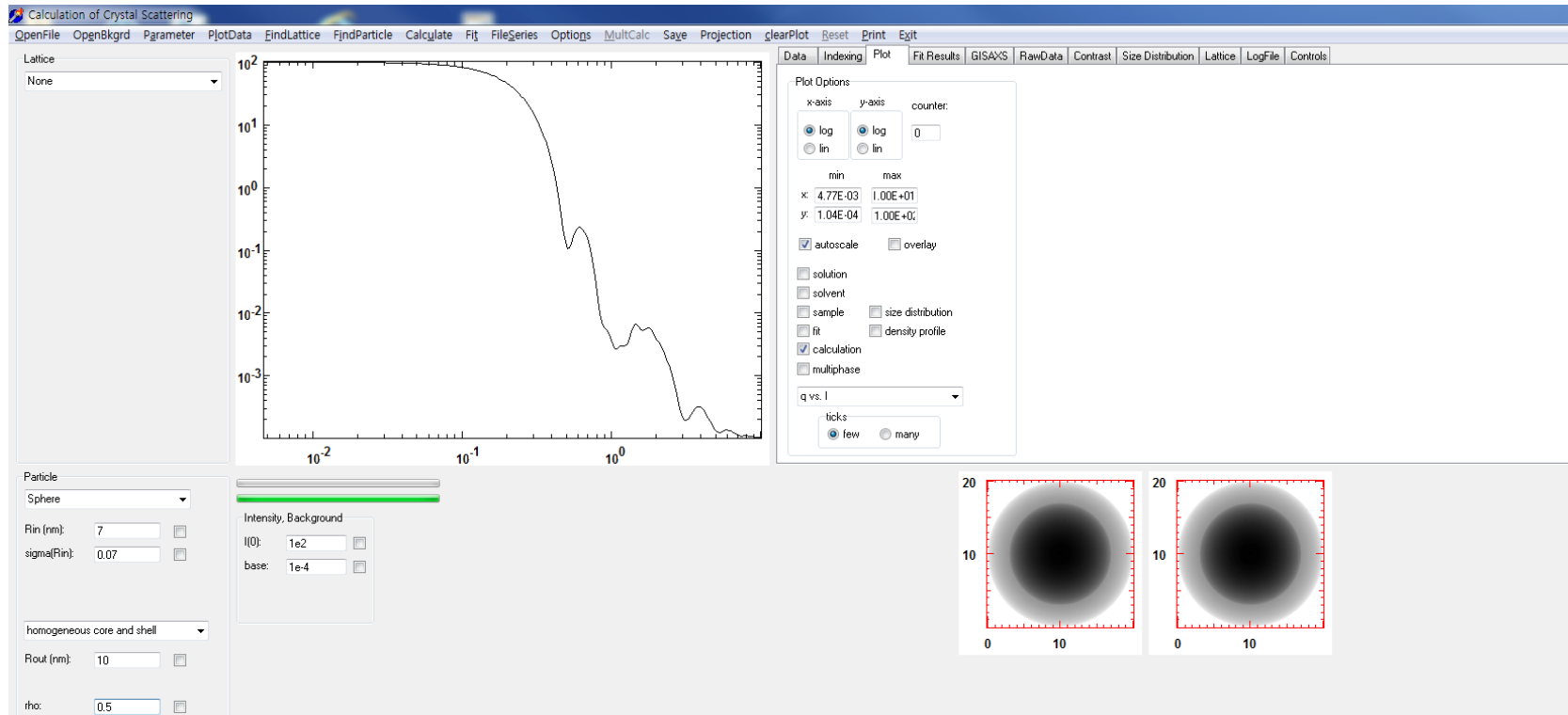
1.7. Model Independent Approach: Ab initio methods



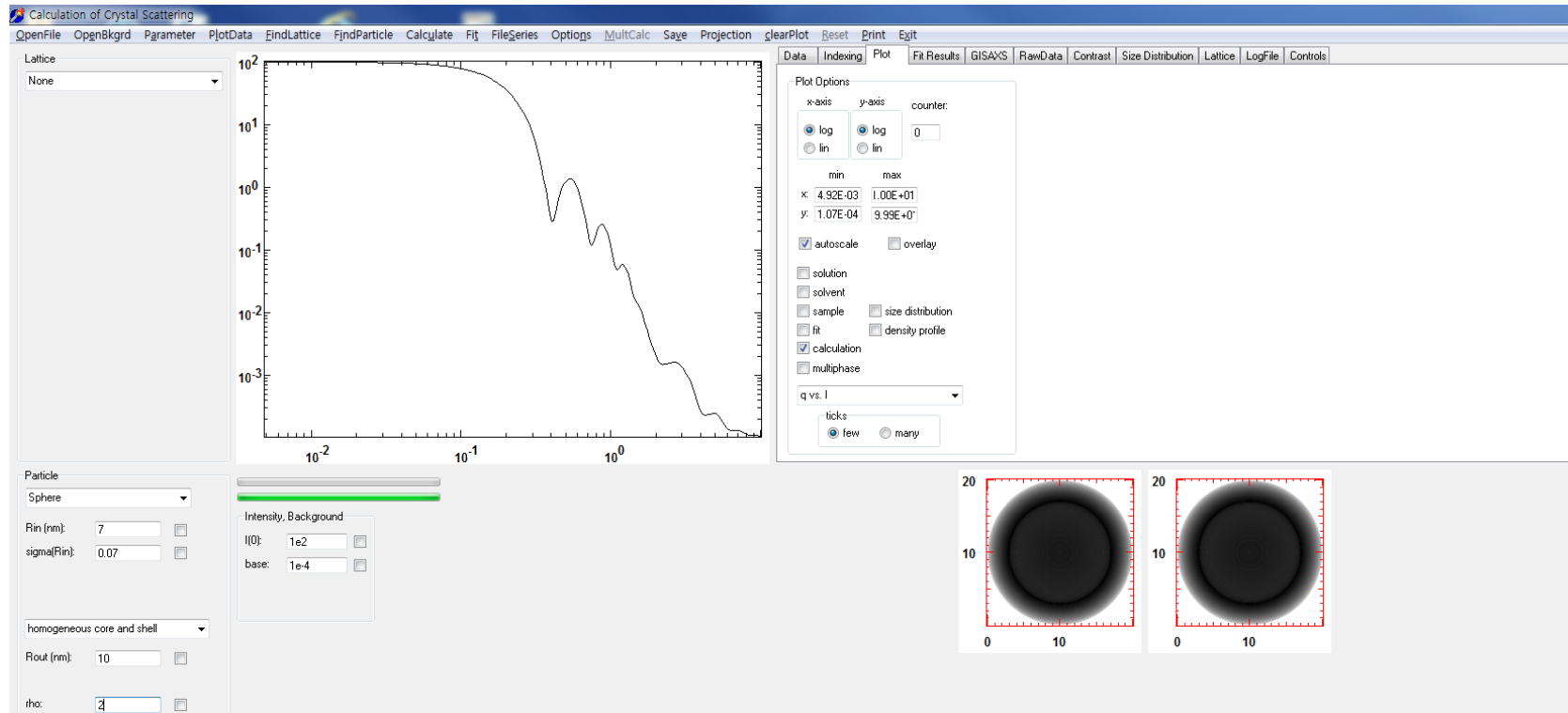
2.1. Model Dependent Approach: Sphere Model



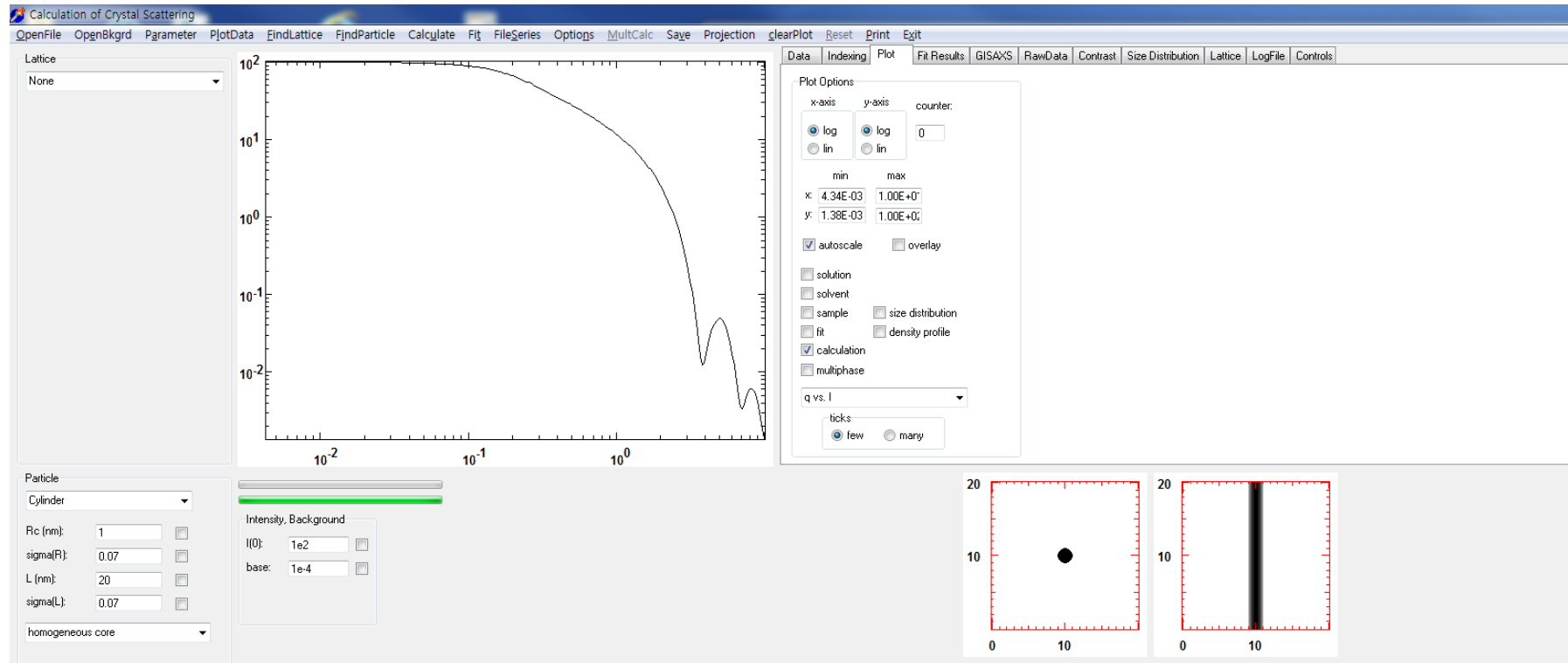
2.2. Model Dependent Approach: Core-shell Model



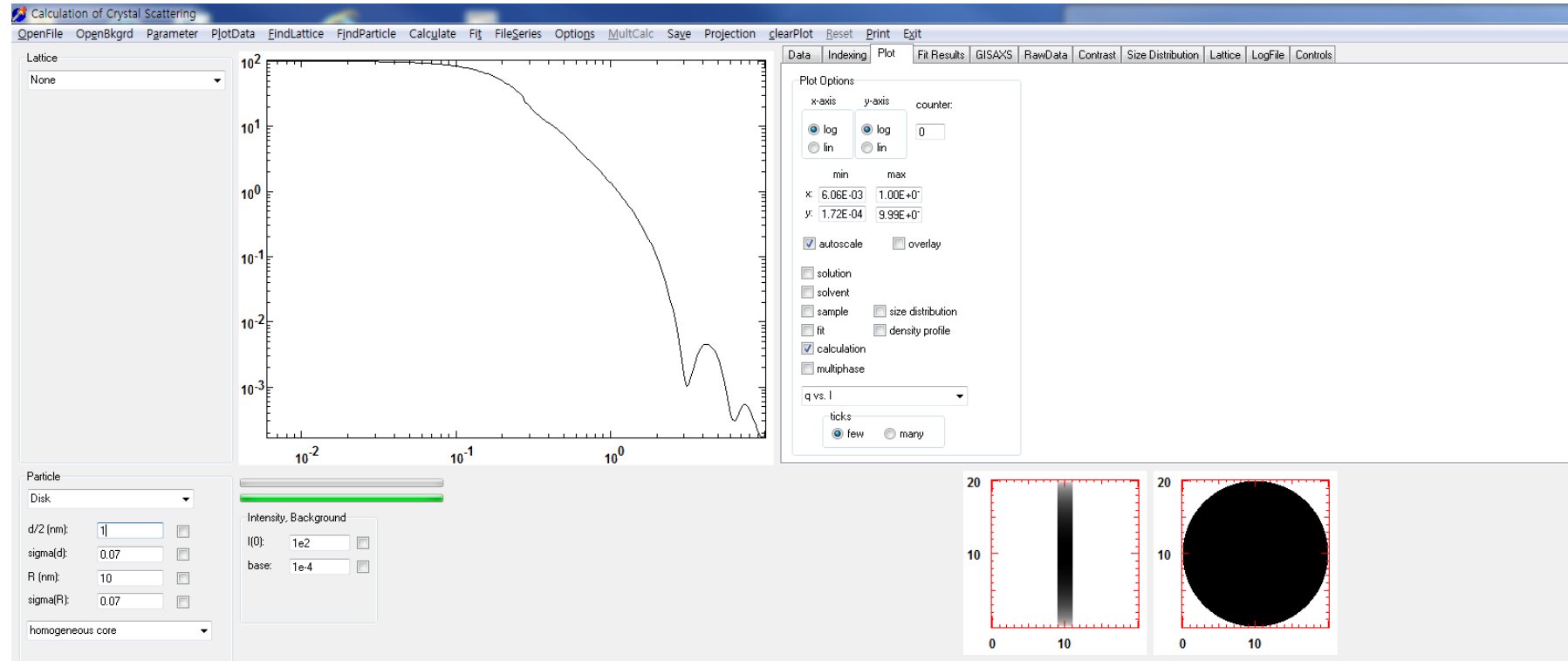
2.3. Model Dependent Approach: Core-shell Model



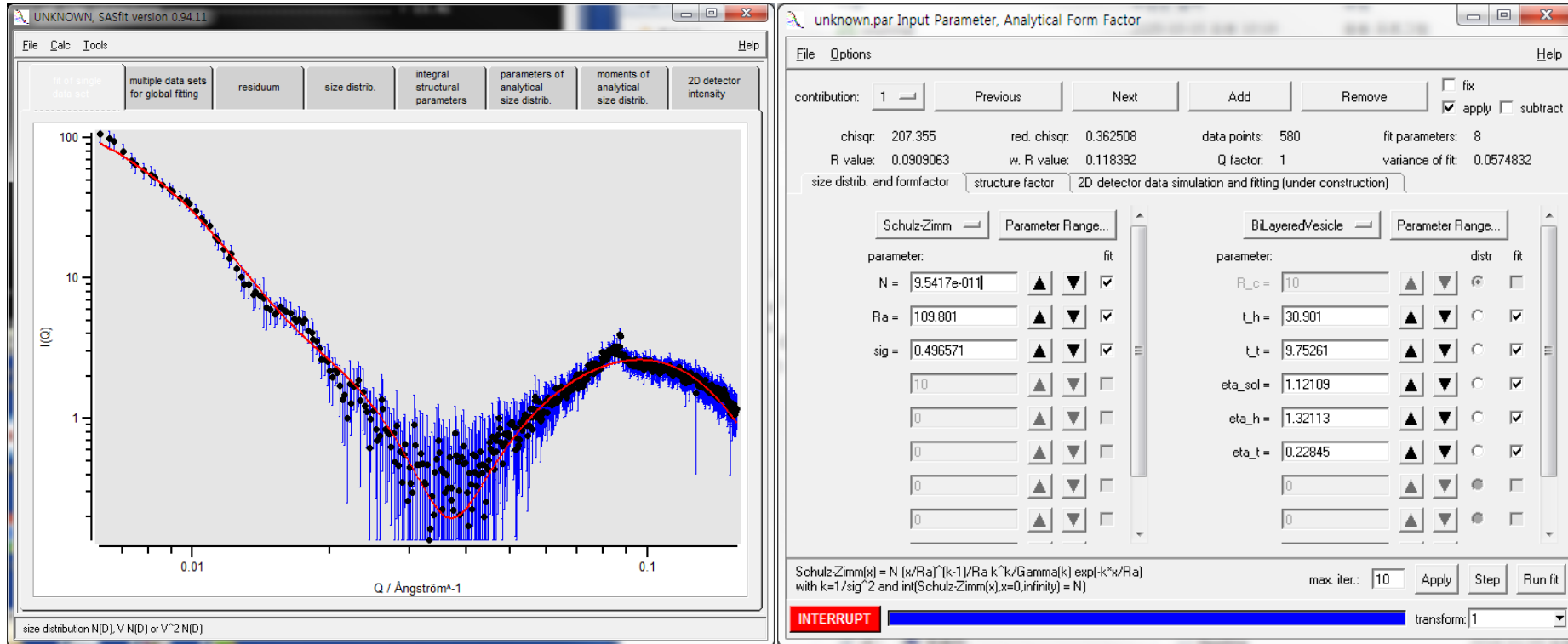
2.4. Model Dependent Approach: Cylinder Model



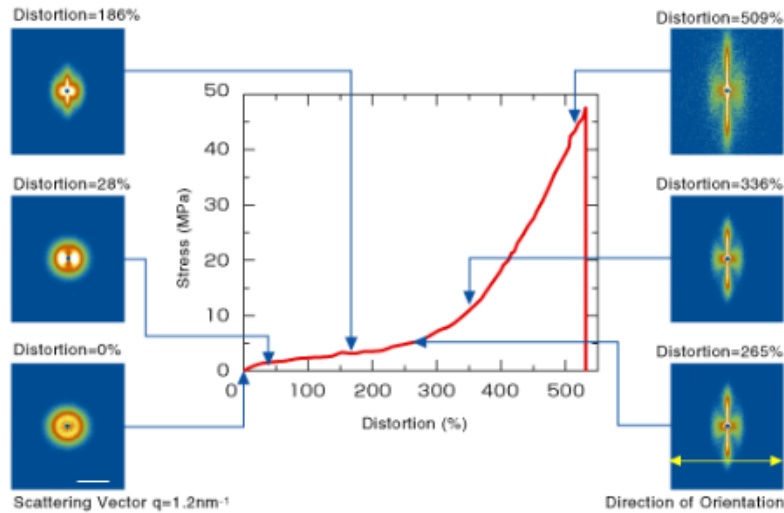
2.5. Model Dependent Approach: Disk Model



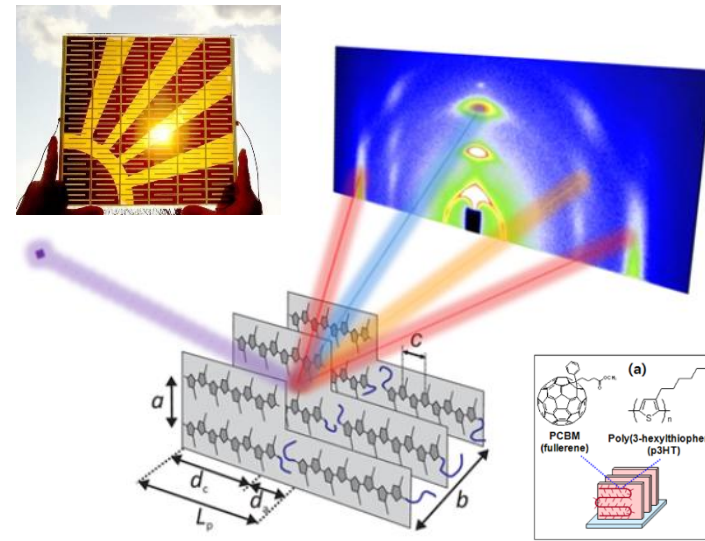
2.6. Model Dependent Approach: Bilayered Vesicle Model



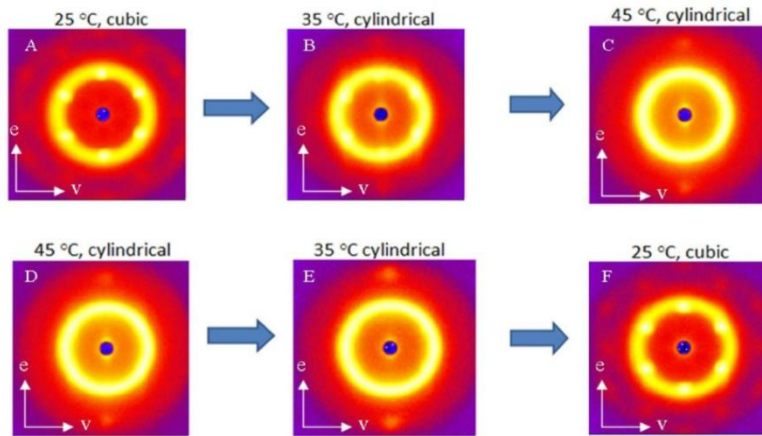
Bilayered vesicle model
 (Thickness of outer part of bilayer=3nm, Thickness of inner part of bilayer=1nm, R=10nm)



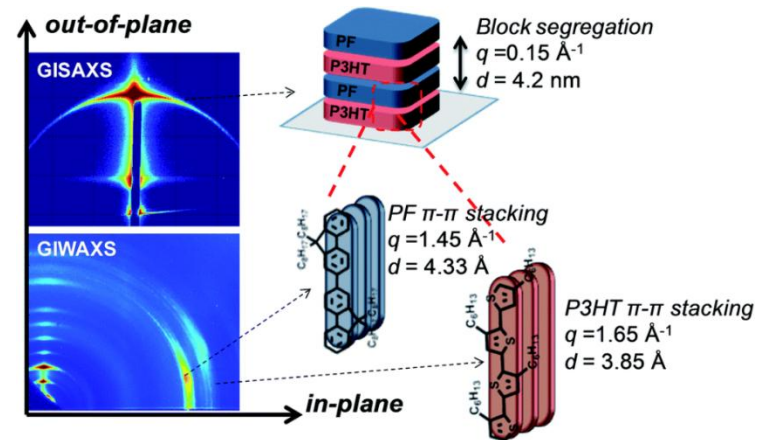
타이어의 응력-변형을 연구



태양광 전지 (Organic Solar Cells)

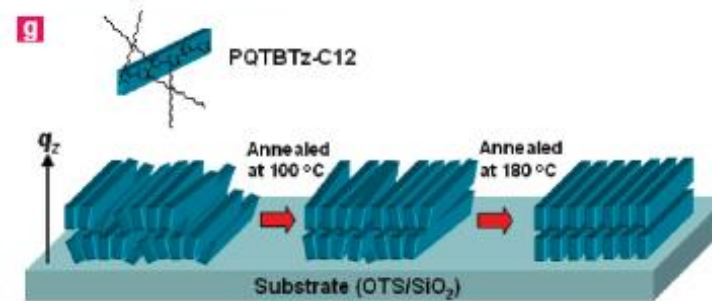
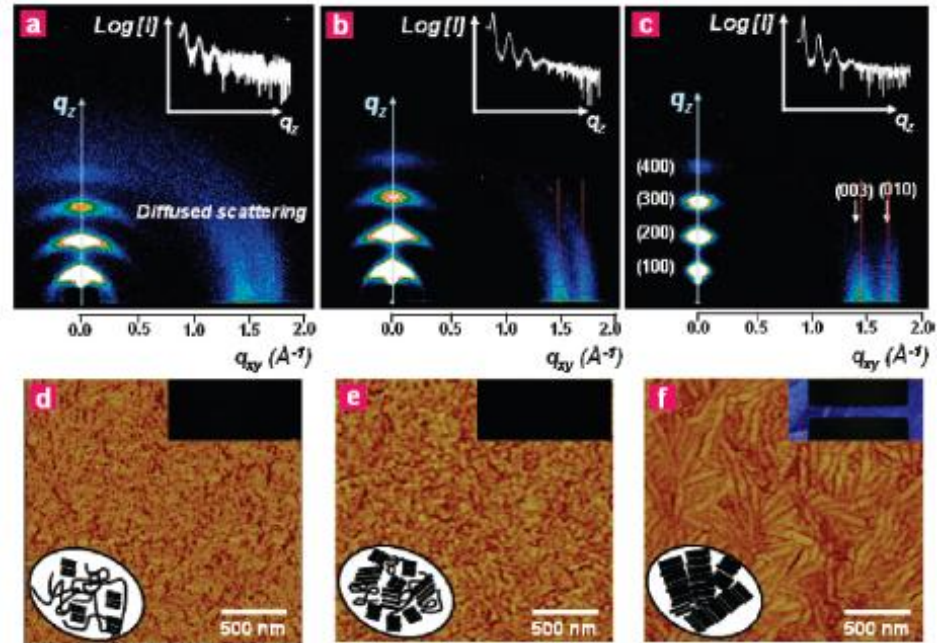


블록공중합체 고분자의 구조/역학적 이력 연구



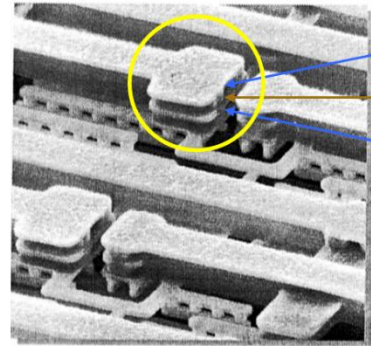
용매 어닐링 처리 액정 고분자의 구조 연구

Flexible Display Application: Organic Thin-film Transistor

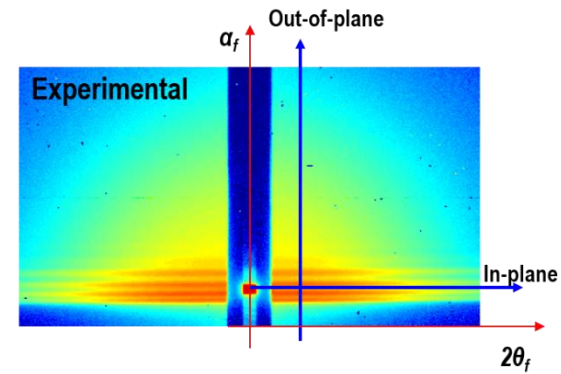
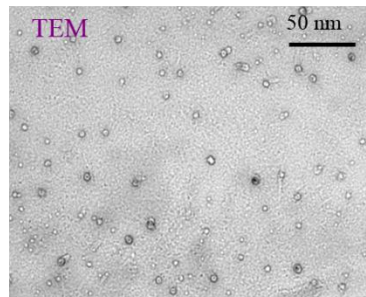
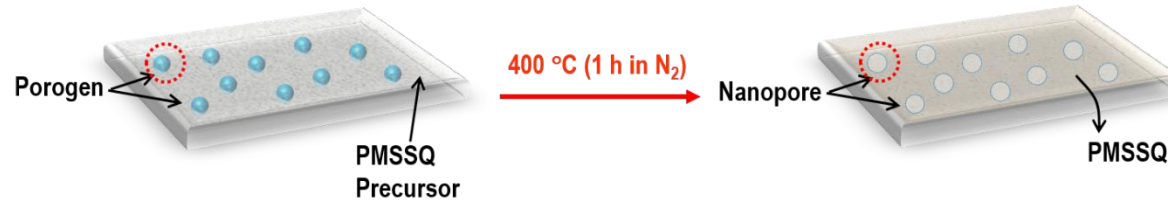
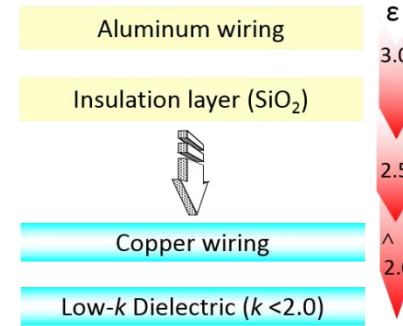


Journal of the American Chemical Society (2009)

Ultra-low-K Dielectrics in Nano-thin-films

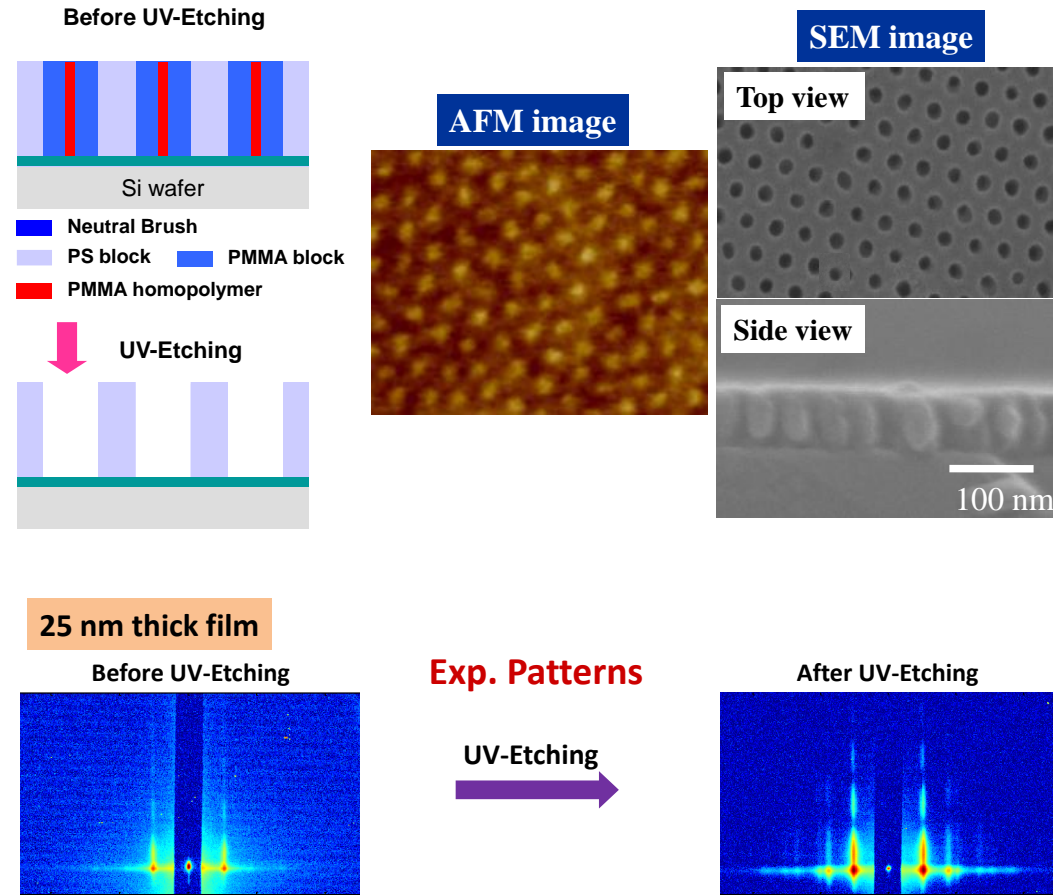


Upper metal layer
Insulator
Lower metal layer



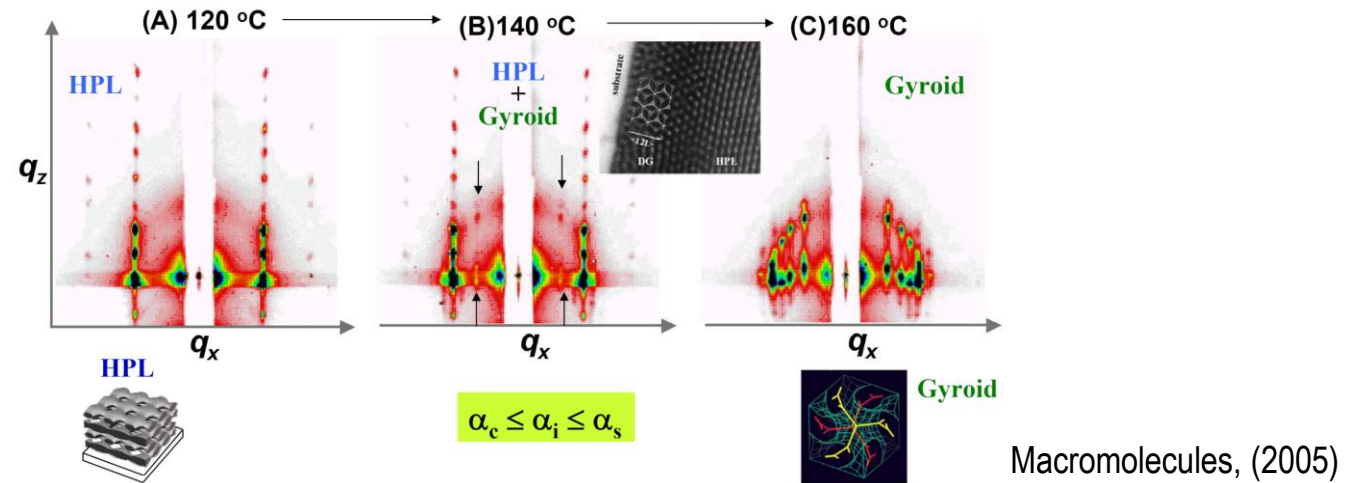
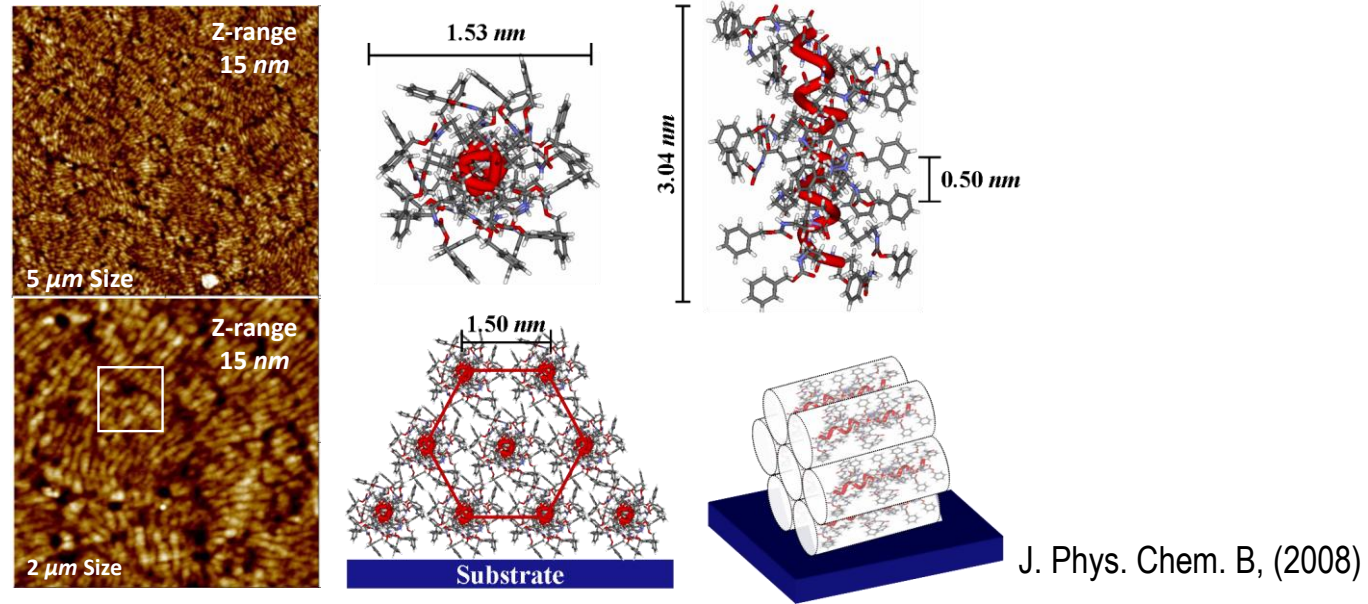
Nat. Mater. 4, 147 (2005), Adv. Mater. 17, 696 (2005), Macromolecules 2005, 38, 4311-4323, J. Appl. Cryst. 2008, 41, 281-291

Nano-templates: Ultra-fine Filter Membranes

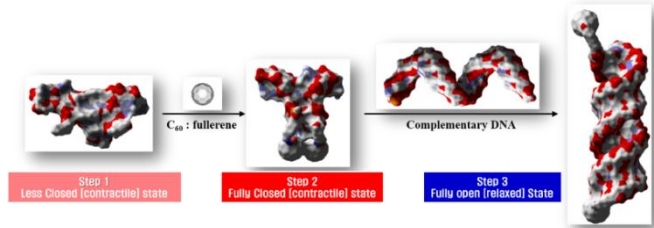


Adv. Funct. Mater., 18, 1371 (2008)

Polymer Nanostructure

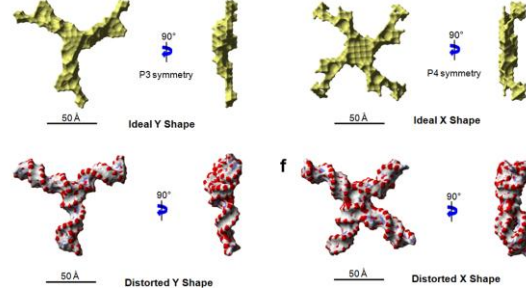


1. Proton-sensitive DNA



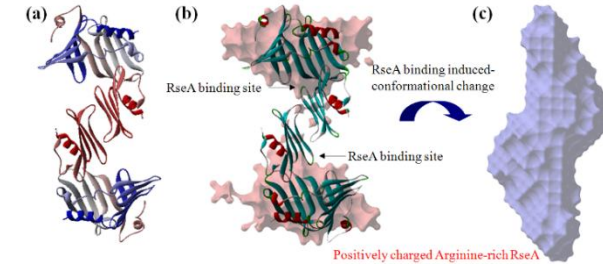
Adv. Mater. 2009, 21, 1907-1910.

2. Branched DNA Molecule



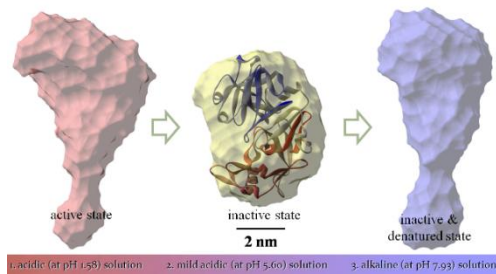
Scientific Reports 2013, 3, 3226

3. Stress-related RseA/RseB Protein



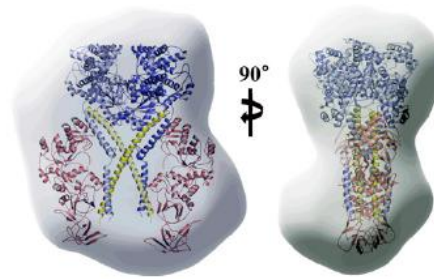
PNAS 2007, 104, 8779-8784.

4. Digestion-related Pepsin Protein



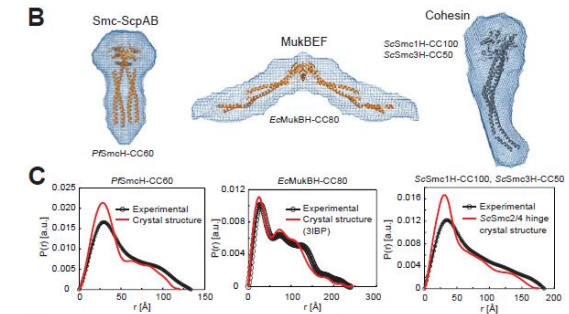
J. Phys. Chem. B 2008, 112, 15821-15827.

5. Mammalian Translation-related Protein



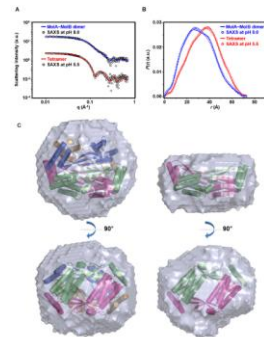
PNAS 2014, 111, 15084-15089.

6. Chromosome-related SMC Protein



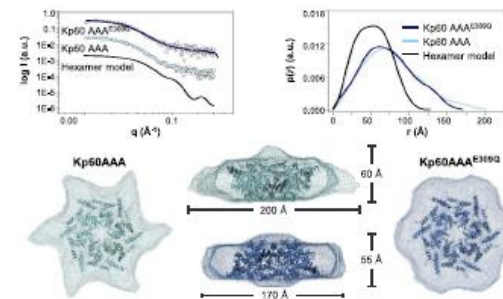
Molecular Cell 2015, 57, 290-303.

7. Pathogenic Bacteria-related Protein



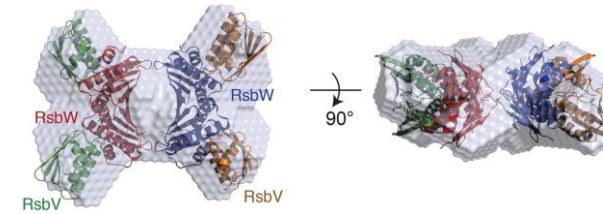
Frontiers in Microbiology 2019, 9, 3329.

8. Microtubule (MT)-severing Enzyme



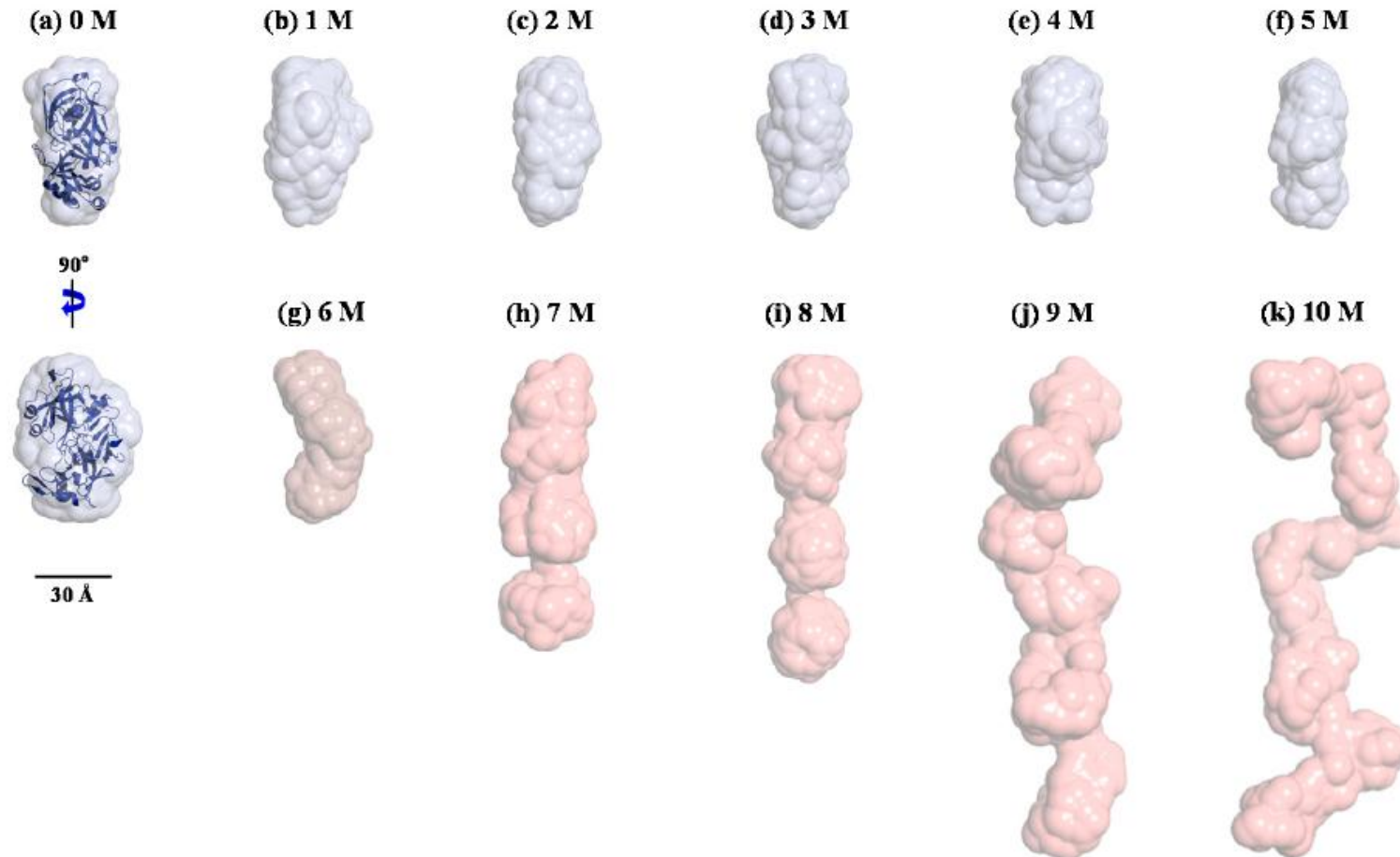
Cell Reports 2019, 26, 1357-1367.

9. Stress-related RseV/RseW Protein



IUCrJ 2020, 7, 737-747.

GASBOR *ab initio* Envelope of Pepsin in Solution



Structural models of pepsin in solution under various denaturing conditions with 0–10 M urea (a–k, respectively) using the *ab initio* shape method program GASBOR. Surface rendering in the structural model was achieved using the program PyMOL. For the comparison of overall shapes and dimensions, the ribbon diagrams of the atomic crystal structure of pepsin were superimposed on the reconstructed dummy residues models using SUPCOMB (NSD = 1.802).

“Chemically Denatured Structures of Porcine Pepsin using Small-Angle X-ray Scattering” *Polymers* **2019**, 11(12), 2104

Liquid Crystalline Lipid Nanoparticles

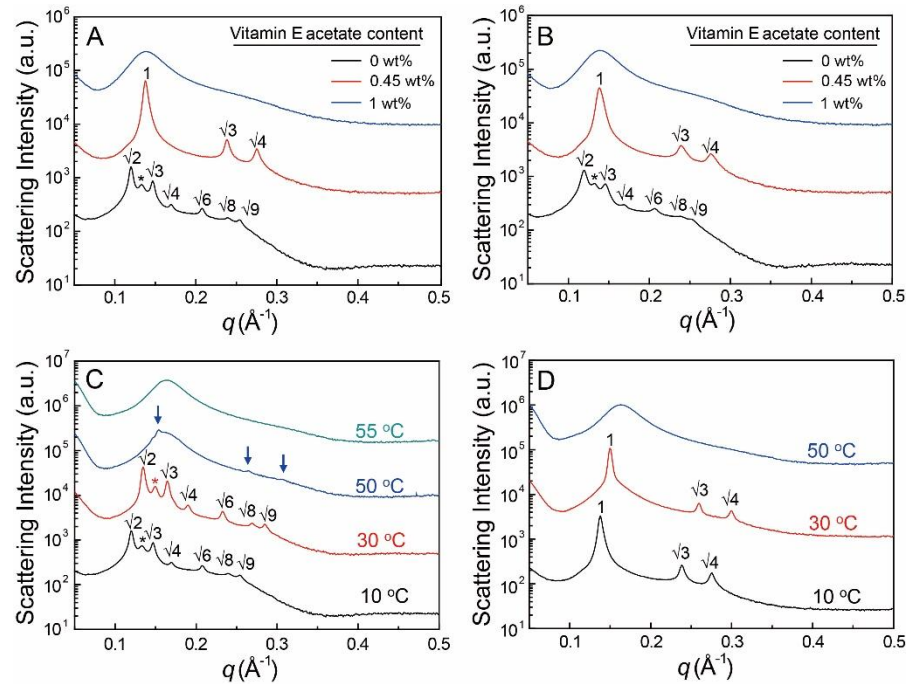
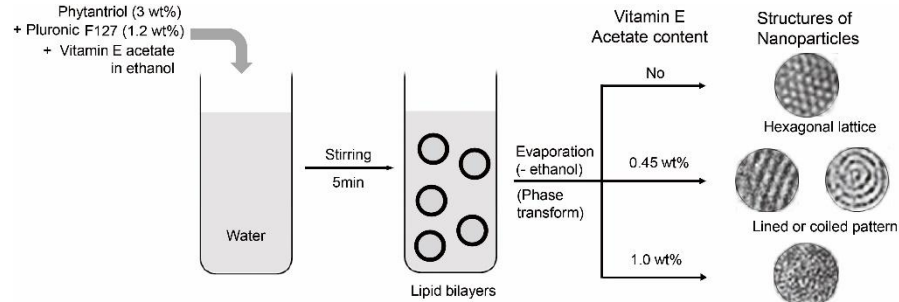


Table 2. Structural parameters obtained from the SAXS data (Figure 5) of the liquid nanoparticles.

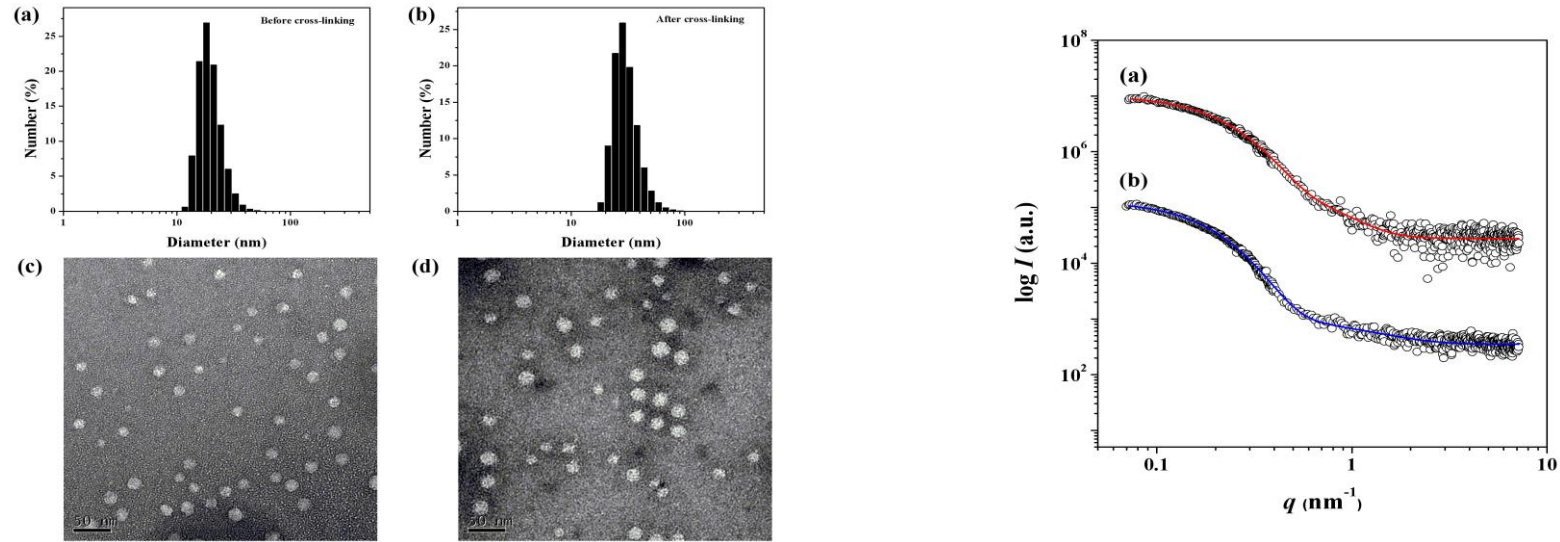
Preparation Method	Vitamin E Acetate Concentration (wt%) ^{c)}	Space Group	Lattice Parameter, a (Å)		
Evaporation Method ^{a)}	0	10 °C ^{d)}	$Pn\bar{3}m$ H_2 74.1 ± 0.2 - ^{e)}		
		30 °C	$Pn\bar{3}m$ H_2 66.0 ± 0.2 - ^{e)}		
		50 °C	H_2 L_2 47.4 ± 0.2 38.9 ± 0.3 ^{f)}		
	0.45	55 °C	L_2 38.3 ± 0.3 ^{f)}		
		10 °C	H_2 52.8 ± 0.3		
		30 °C	H_2 48.5 ± 0.3		
		50 °C	L_2 38.5 ± 0.3 ^{f)}		
		1.0	10 °C	L_2 45.3 ± 0.3 ^{f)}	
		Conventional Method (Ref. 16) ^{b)}	0	10 °C	$Pn\bar{3}m$ H_2 74.3 ± 0.3 - ^{e)}
			0.45	10 °C	H_2 52.6 ± 0.3
1.0	10 °C		L_2 45.1 ± 0.3 ^{f)}		

- a) The method developed from the present study.
- b) The method from Ref. 16.
- c) For all the samples, the concentrations of phytantriol and F127 were 3.0 and 1.2 wt%, respectively, in the aqueous dispersion.
- d) Measurement temperatures
- e) Lattice parameters were not determined due to lack of second and third peaks. See the text for the explanation.
- f) The characteristic distance for the L_2 phase ($d = 2\pi/q$) from the observed single broad peak.

Collaboration : Prof. Eun Chul Cho (Amorepacific & Hanyang Univ.)

Do-Hoon Kim, Sora Lim, Jongwon Shim, Ji Eun Song, Jong Soo Chang, Kyeong Sik Jin* and Eun Chul Cho* *ACS Applied Materials & Interfaces* **2015**, 7, 20438-20446

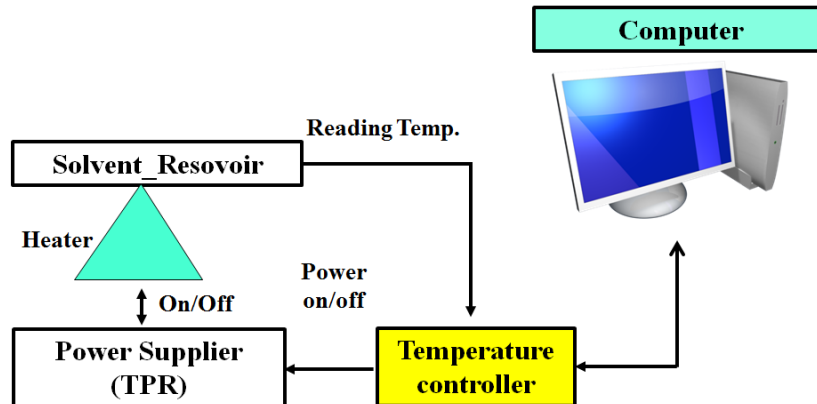
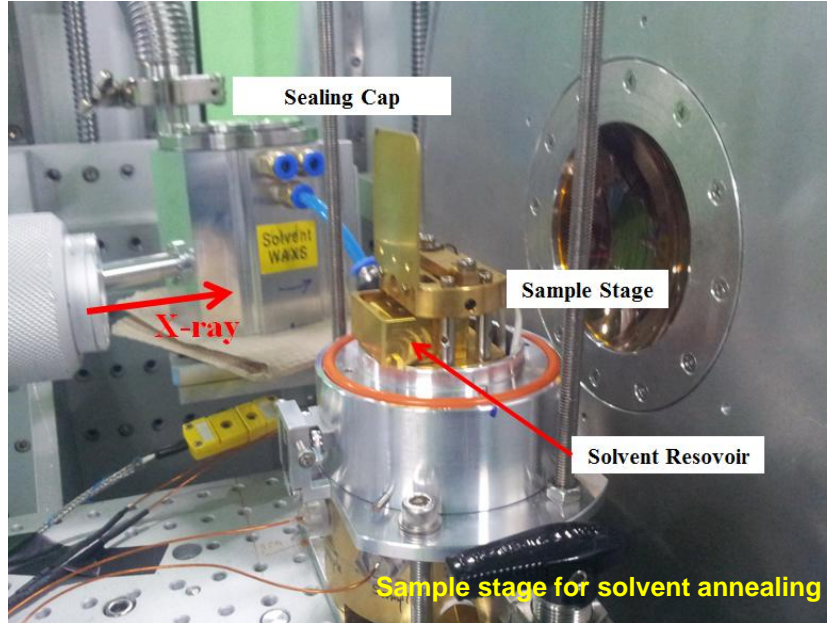
Cross-linked Polymer Micelles



Sample	NCPMs		CPMs	
Model	sphere		sphere	
Type	homogeneous core and shell		homogeneous core and shell	
^a R _c (nm)	3.220	^b (4.317)	1.460	^b (1.914)
^c σ _R	0.326	-	0.322	-
^d R _{c, max} (nm)	2.888	^e (3.944)	1.228	^e (1.732)
^f R _m (nm)	11.90	^g (15.69)	13.70	^g (17.96)
^h R _{m, max} (nm)	10.61	ⁱ (14.48)	12.21	ⁱ (16.40)
^j Rho	0.106	-	0.019	-

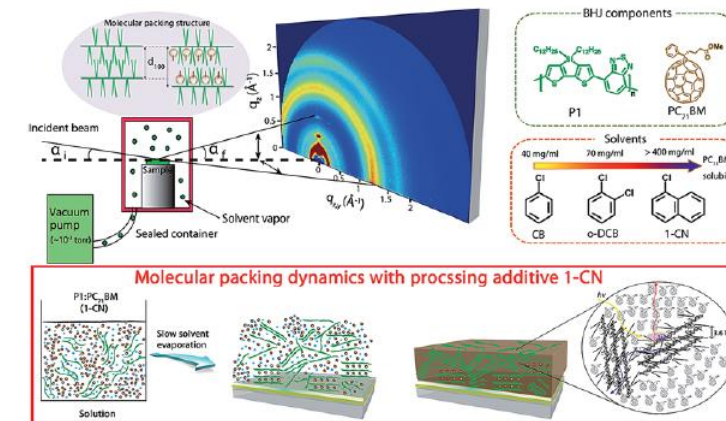
Hyun-Chul Kim*, Kyeong Sik Jin*, Se Guen Lee, Eunjoo Kim, Sung Jun Lee, Sang Won Jeong, Seung Woo Lee, and Kwang-Woo Kim. *Journal of Nanoscience and Nanotechnology* **2016**, 16, 6432-6439. Collaboration : Dr. Hyun-Chul Kim (DGIST)

Solvent Vapor Adsorption Device (at 3C BL)



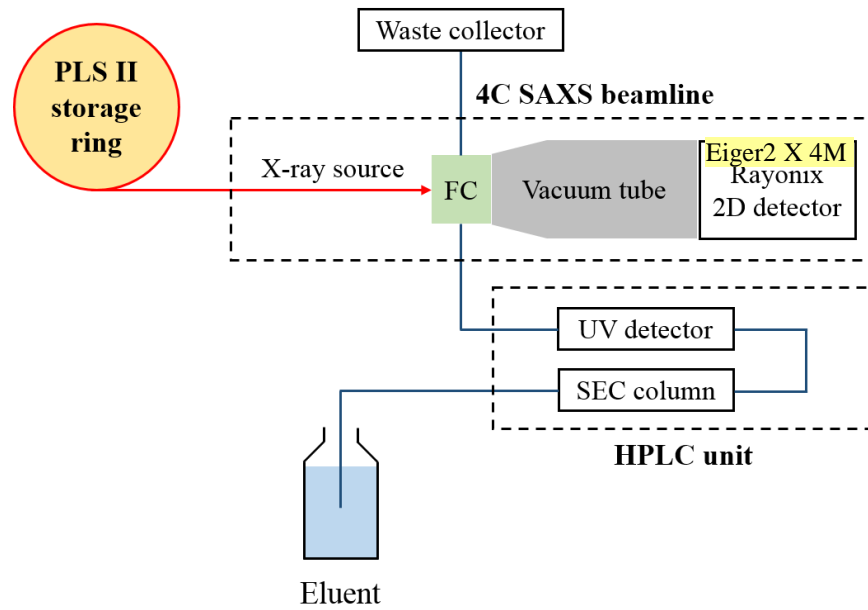
Design Criteria

Temperature range : 20 °C ~ 250 °C
Solvent Reservoir : 20x20x5 mm³

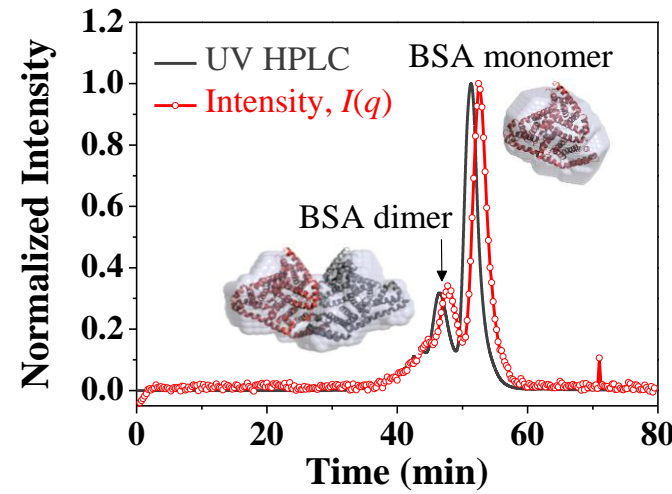
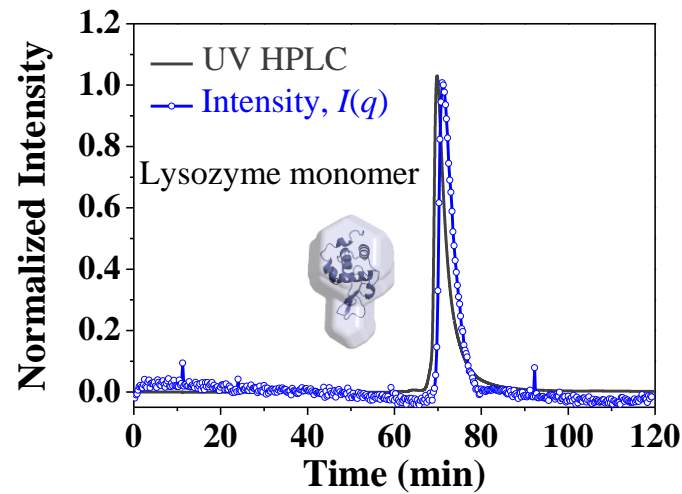


“ In-situ Studies of Molecular Packing Dynamics of Bulk-heterojunction Solar Cells induced by the Processing Additive 1-Chloronaphthalene” **Journal of Materials Chemistry A**, 2015, (DOI: 10.1039/C5TA00833F)

Size-exclusion Chromatography (SEC)-SAXS (at 4C BL)



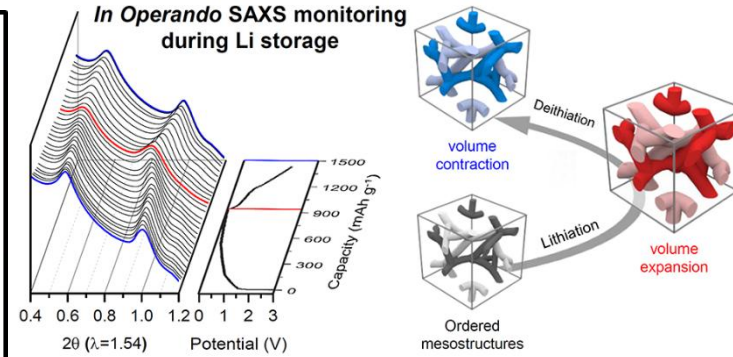
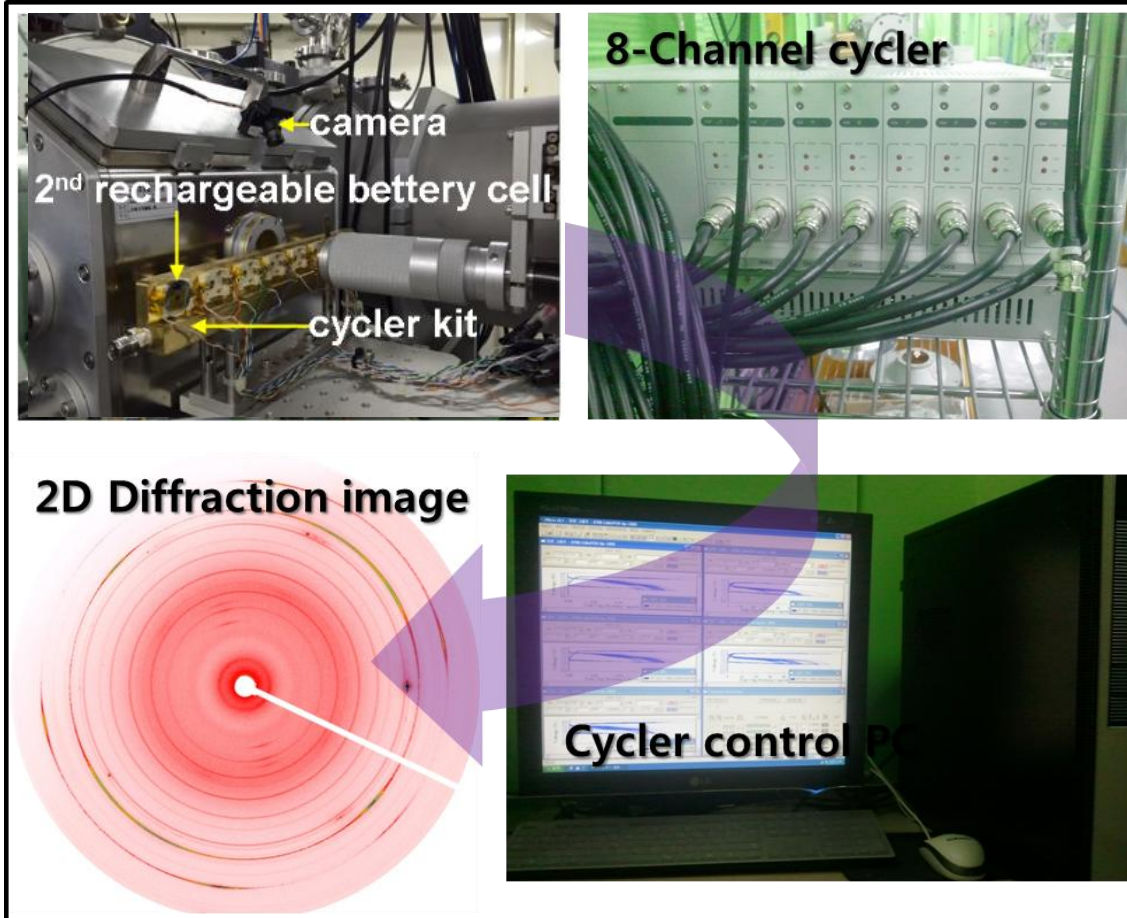
[Agilent 1260 Infinity HPLC System]



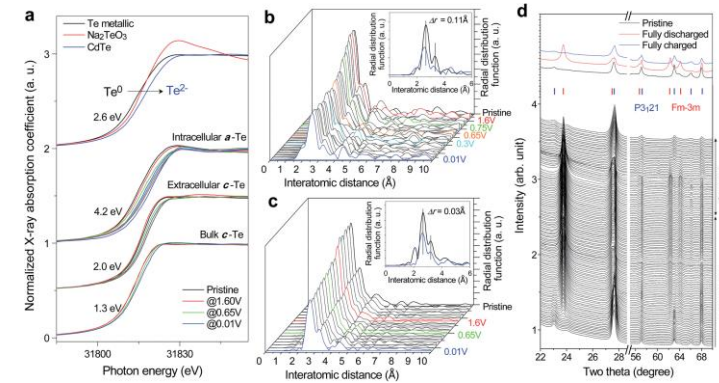
B. Kor. Chem. Soc., (2020)

in-situ Experiment (Tr-mode) : Battery Cycling (at 6D BL)

in-situ Cycling : EXAFS, WAXD, SAXS



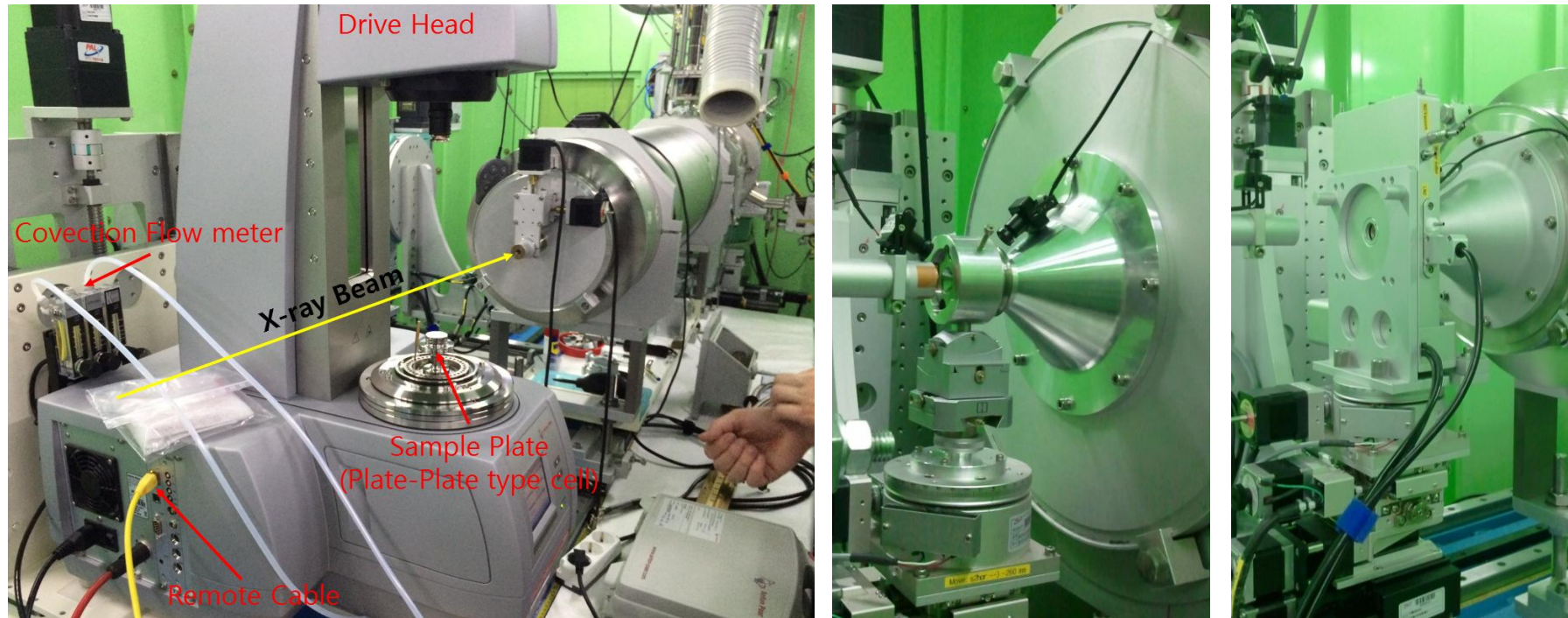
ACS nano 2015, 5, 5470–5477, Y. S. Youn et. Al.



Li-ion storage through anionic redox processes of bacteria-driven tellurium nanorods,

J. Mater. Chem. A, 2015, 3, 16978, M.G. Kim et. al.

Rheo-, High Pressure-, and Tensile Stress SAXS (at 9A BL)



Thank you for your attention

